Statistical characterization of erosion and sediment transport mechanics in shallow tidal environments. Part 1: erosion dynamics

Andrea D'Alpaos[1], Davide Tognin[1], Laura Tommasini[2], Luigi D'Alpaos[1], Andrea Rinaldo[3], and Luca Carniello[4]

[1]University of Padova
[2]Department fof Geosciences, University of Padova
[3]École Polytehnique Fédérale de Lausanne EPFL
[4]Department of Civil, Environmental, and Architectural Engineering, University of Padova

February 21, 2023

Abstract

Wave-induced bottom shear stress is one of the leading processes that control sediment erosion dynamics in shallow tidal environments, because it is responsible for sediment resuspension and, jointly with tidal currents, for sediment reworking on tidal flats. Reliable descriptions of erosion events are foundational to effective frameworks relevant to the fate of tidal landscape evolution. However, the absence of long-term, measured time series of bottom shear stress (BSS) prevents a direct analysis of erosion dynamics. Here we adopted a fully-coupled, bi-dimensional numerical model to compute BSS generated by both tidal currents and wind waves in six historical configurations of the Venice Lagoon in the last four centuries. The one-year-long time series of the total BSS were analyzed based on the peak-over-threshold theory to statistically characterize events that exceed a given erosion threshold and investigate the effects of morphological modifications on spatial and temporal erosion patterns. Our analysis suggests that erosion events can be modeled as a marked Poisson process in the intertidal flats for all the considered configurations of the Venice Lagoon, because interarrival times, durations and intensities of the over-threshold exceedances are well described by exponentially distributed random variables. Moreover, while the intensity and duration of over-threshold events are temporally correlated, almost no correlation exists between them and interarrival times. The resulting statistical characterization allows for a straightforward computation of morphological indicators, such as erosion work, and paves the way to a novel synthetic, yet reliable, approach for long-term morphodynamic modeling of tidal environments.

Statistical characterization of erosion and sediment transport mechanics in shallow tidal environments. Part 1: erosion dynamics

Andrea D'Alpaos[1,*], Davide Tognin[1,2,*], Laura Tommasini[1], Luigi D'Alpaos[2], Andrea Rinaldo[2,3], and Luca Carniello[2]

[1]Department of Geosciences, University of Padova, Padova, Italy
[2]Department of Civil, Environmental, and Architectural Engineering, University of Padova, Padova, Italy
[3]Laboratory of Ecohydrology ECHO/IEE/ENAC, Ècole Polytechnique Fèdèrale de Lausanne, Lausanne, Switzerland
[*]These authors contributed equally to this work.

Correspondence: Davide Tognin (davide.tognin@unipd.it)

Abstract. Wave-induced bottom shear stress is one of the leading processes that control sediment erosion dynamics in shallow tidal environments, because it is responsible for sediment resuspension and, jointly with tidal currents, for sediment reworking on tidal flats. Reliable descriptions of erosion events are foundational to effective frameworks relevant to the fate of tidal landscape evolution. However, the absence of long-term, measured time series of bottom shear stress (BSS) prevents a direct analysis of erosion dynamics. Here we adopted a fully-coupled, bi-dimensional numerical model to compute BSS generated by both tidal currents and wind waves in six historical configurations of the Venice Lagoon in the last four centuries. The one-year-long time series of the total BSS were analyzed based on the peak-over-threshold theory to statistically characterize events that exceed a given erosion threshold and investigate the effects of morphological modifications on spatial and temporal erosion patterns. Our analysis suggests that erosion events can be modeled as a marked Poisson process in the intertidal flats for all the considered configurations of the Venice Lagoon, because interarrival times, durations and intensities of the over-threshold exceedances are well described by exponentially distributed random variables. Moreover, while the intensity and duration of over-threshold events are temporally correlated, almost no correlation exists between them and interarrival times. The resulting statistical characterization allows for a straightforward computation of morphological indicators, such as erosion work, and paves the way to a novel synthetic, yet reliable, approach for long-term morphodynamic modeling of tidal environments.

1 Introduction

Wind waves are key drivers of the morphological evolution of shallow tidal landscapes (Green and Coco, 2014). The morphology of tidal flats and subtidal platforms is mainly controlled by wave-induced erosion and resuspension, together with the rate of relative sea level rise and sediment supply (Fagherazzi et al., 2006; D'Alpaos et al., 2012; Hu et al., 2017; Zhou et al., 2017; Belliard et al., 2019). Moreover, the action of wind waves is usually recognized as one of the main causes of the retreat of salt-marsh margins (Möller et al., 1999; Schwimmer, 2001; Marani et al., 2011; Bendoni et al., 2016; Leonardi et al., 2016; Finotello et al., 2020). Therefore, the temporal and spatial evolution of wave-induced bottom shear stresses (BSSs) has an important impact on sediment dynamics in the intertidal zone (Carniello et al., 2005; Fagherazzi and Wiberg, 2009;

Mariotti et al., 2010), ultimately influencing the morphological and biological processes responsible for the evolution of tidal systems. For instance, local wave-induced BSS can influence sediment winnowing and distribution on tidal flats (Zhou et al., 2015; Ghinassi et al., 2019). Moreover, large wave-induced BSSs can disrupt the polymeric biofilm built up by microphytobenthos (MPB) typically colonizing the bed sediment in shallow tidal environments (Amos et al., 2004; Mariotti and Fagherazzi, 2012), and therefore promote erosion of tidal-flat surfaces. The related increase in suspended sediment concentration (SSC) can trigger negative feedback by promoting the decrease of light availability in the water column and thus limiting the seagrass and MPB proliferation (Lawson et al., 2007; Carr et al., 2010; Chen et al., 2017; Pivato et al., 2019). However, at the same time, increased SSC, typically occurring during storm surges, can support sedimentation on salt marshes, thus helping them to keep pace with sea level rise (Goodbred and Hine, 1995; Tognin et al., 2021). Therefore, understanding BSS dynamics is fundamental to describe to morphodynamic evolution of tidal flats and to indicate long-term sustainable management strategies for shallow tidal systems (Zhou et al., 2022), which is crucial under the increasing pressure of relative sea level rise (Nicholls et al., 2021) and human interventions (Tognin et al., 2022).

The wind-wave and the related BSS fields, as well as their impact on the morphodynamics of shallow tidal basins, can be provided by several numerical models. However, modeling the morphodynamic evolution over time scales of centuries using fully-fledged models is a difficult task due to the computational burden involved and, therefore, simplified approaches are more and more frequently adopted (Murray, 2007). Opting for such a simplified approach, long-term models ideally should be tested in tidal systems where information on the morphological evolution is available for a sufficiently long time. From this point of view, the Venice Lagoon, Italy (Figure 1) represents an almost unique opportunity to test long-term models, because several bathymetric surveys are available for the last four centuries (Carniello et al., 2009; Tommasini et al., 2019; Finotello et al., 2022).

Towards the goal of developing a synthetic theoretical framework to represent wind-wave-induced erosion events and accounting for their influence on the long-term morphodynamic evolution of tidal systems, we applied a two-dimensional finite element model for reproducing and analysing the combined effect of wind waves and tidal currents in generating BSSs in several historical configurations of the Venice Lagoon. More in detail, in the present study, we used the fully coupled Wind Wave-Tidal Model (WWTM) (Carniello et al., 2005, 2011) to investigate the hydrodynamic behaviour in six historical configurations of the Venice Lagoon, namely 1611, 1810, 1901, 1932, 1970, and 2012. For each configuration, we run a one-year-long simulation considering representative tidal and meteorological boundary conditions. The resulting spatial and temporal dynamics of BSSs for the six selected configurations were analyzed on the basis of the peak-over-threshold (POT) theory once a critical shear stress for bed sediment erosion was chosen.

The main goal of this analysis is to find whether, in line with previous results on the nowadays configuration of the Venice Lagoon (D'Alpaos et al., 2013), wave-induced erosion events can be modeled as marked Poisson processes also in different morphological settings. The relevance of this result lies in the possibility of describing erosion processes as a Poisson process over time, which represents a promising framework for long-term studies. Indeed, the analytical characterization of the long-term behaviour of geophysical processes is becoming increasingly popular in hydrology and geomorphology (e.g., Rodriguez-Iturbe et al., 1987; D'Odorico and Fagherazzi, 2003; Botter et al., 2007; Park et al., 2014), although the applications to tidal landscapes are still quite rare (D'Alpaos et al., 2013; Carniello et al., 2016). Our analyses provide a temporally and spatially explicit characterization of wind-induced erosion events for the Venice Lagoon starting from the beginning of the seventeenth century, thus allowing us to investigate and understand the main features of the erosive trends the lagoon has been experiencing and to provide predictions on future scenarios.

2 Materials and Methods

2.1 Geomorphological setting

The Venice Lagoon, located in the northern Adriatic Sea and characterized by an area of 550 km^2, formed over the last 7500 years covering alluvial Late Pleistocene, silty-clayey deposits, locally known as Caranto (Zecchin et al., 2008). In the present-day morphology, the lagoon is connected to the sea with three inlets, namely Lido, Malamocco, and Chioggia (Figure 1), through which the semidiurnal tide with a maximum tidal oscillation of about 0.75 m typical of the northern Adriatic Sea propagates within the lagoon (D'Alpaos et al., 2013). Meteorological conditions also importantly affect the hydrodynamics of the Venice Lagoon. In particular, storm surges generated by the south-easterly Sirocco wind (Figure 1b) often overlap astronomical tides, thus increasing water levels (Mel et al., 2014). Whereas, the north-easterly Bora wind (Figure 1b) is mainly responsible for the generation of wind waves and water level set-up, especially in the central and southern portions of the lagoon (Carniello et al., 2009).

The morphology of the Lagoon deeply changed through the last four centuries (Figure 2), especially owing to anthropogenic modifications (D'Alpaos, 2010a). By the end of the 16^{th} century, all the major rivers flowing into the lagoon were diverted to debouch directly into the open sea, thus dramatically decreasing fluvial sediment input. Furthermore, between the 1900s and 1950s, the exploitation of groundwater for industrial purposes accelerated the local subsidence rates, with anthropogenically-induced subsidence reaching values of about 10 to 14 cm in the area of the city of Venice (Carbognin et al., 2004; Zanchettin et al., 2021). In the same period, the total area open to the propagation of tides was largely reduced due to extensive land reclamation carried out to accommodate industrial, agricultural, and aquacultural activities, especially along the landward margin of the lagoon (Figure 2c-e). On the seaward side, massive jetties were built between 1839 and 1934 to stabilize the sections of the three inlets and maintain water depths requested for increasingly bigger commercial ships (Figure 2c,d). For the same reason, navigation channels were excavated in the central part of the lagoon to connect the inner harbour with the sea (Figure 2e). These interventions, together with eustatic sea-level rise (Zanchettin et al., 2021, average value 1.23 ± 0.13 mm/year between 1872 and 2019; 2.76 ± 1.75 mm/year between 1993 and 2019; see), deeply changed the morphological evolution of the lagoon.

We considered six different configurations of the Venice Lagoon (Figure 2 and S1), covering a time span of four centuries, in order to assess the evolution through time of the feedback mechanisms between morphology and wave-induced erosion. The oldest three configurations (1611, 1810, and 1901) were reconstructed by using historical maps, while the more recent ones make use of the topographic surveys carried out by the Venice Water Authority (Magistrato alle Acque di Venezia) in 1932, 1970, and 2003. The updated description of the more recent morphological modifications, which mainly occurred at the three

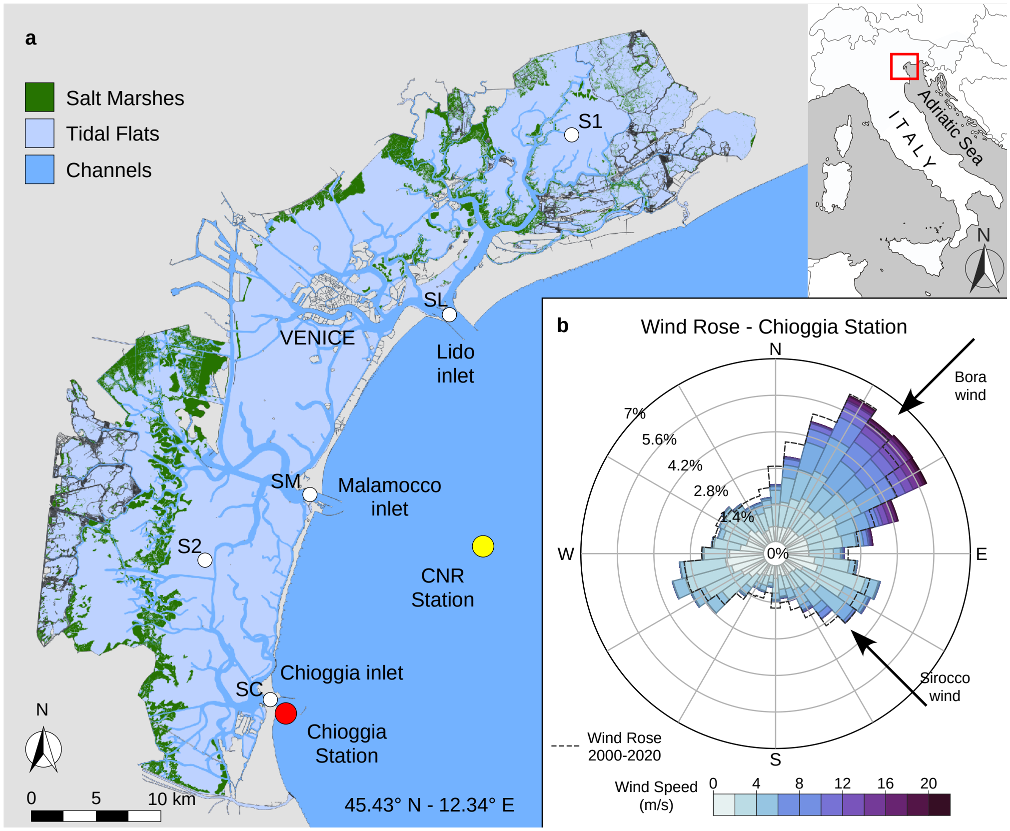

Figure 1. Morphological features and wind conditions characterizing the Venice Lagoon. a, Spatial distribution of the morphological features characterizing the Venice Lagoon. The locations of the anemometric (Chioggia) and oceanographic (CNR Oceanographic Platform) stations are also shown, together with the locations of the three stations at the inlets (SL, SM and SC) and two stations (S1 and S2) for which we provide a detailed statistical characterization of over-threshold events. **b**, Wind rose for the data recorded at the Chioggia station in 2005. Dashed line shows the wind rose for the period 2000-2020.

inlets in the context of the Mo.S.E. project for the safeguard of the city of Venice by high tides (almost completed in 2012), was included in the 2003 configuration, so that we refer to the latter configuration as to the 2012 configuration.

We refer the reader to Tommasini et al. (2019) for a detailed description of the methodology adopted to reconstruct the historical configurations and for information on the bathymetric data of the Venice Lagoon. The computational grids reproducing all the six considered configurations of the Lagoon are shown in Figure S1 and were calibrated in previous studies, namely: 1611 by Tommasini et al. (2019); 1810 by D'Alpaos and Martini (2005) and D'Alpaos (2010b); 1901, 1932, 1970 and 2012 by Carniello et al. (2009) and Finotello et al. (2022).

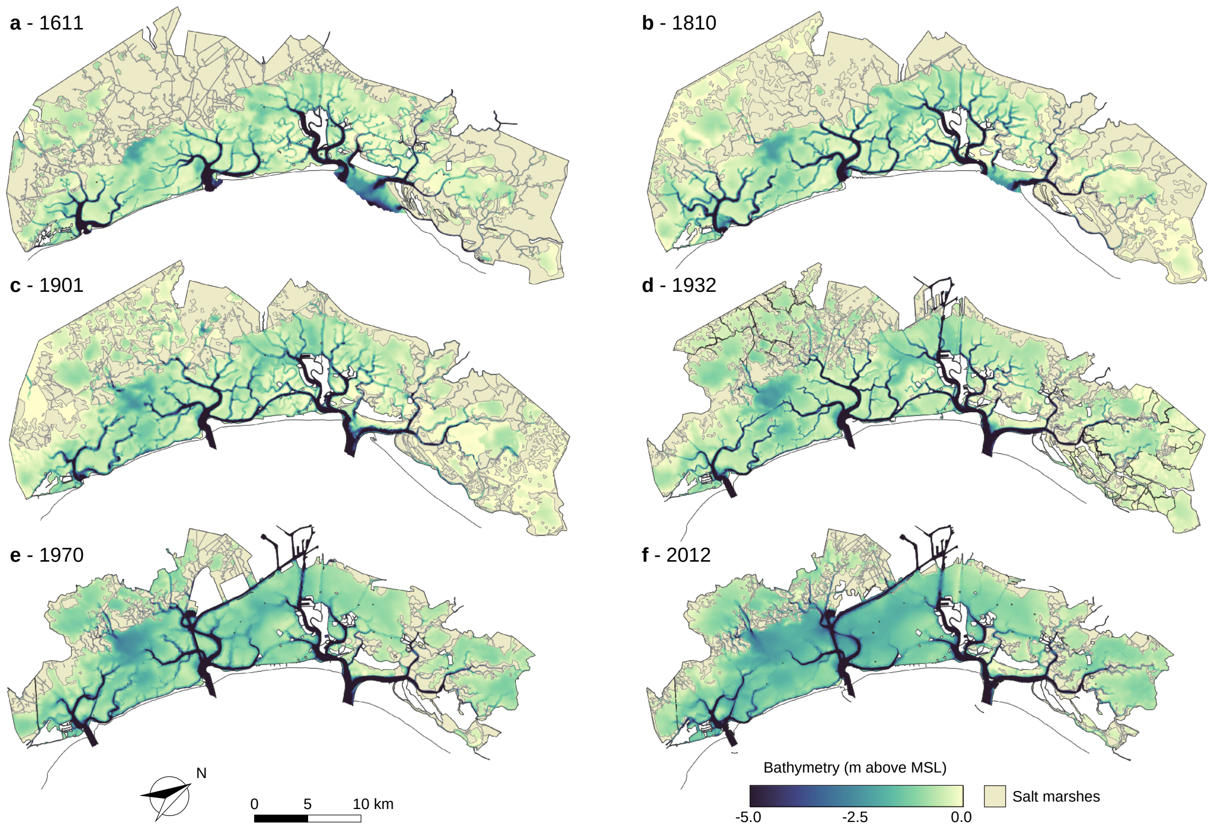

Figure 2. Historical bathymetries of the Venice Lagoon. Color-coded bathymetries of the six different configurations of the Venice Lagoon: 1611 (**a**), 1810 (**b**), 1901 (**c**), 1932 (**d**), 1970 (**e**), and 2012 (**f**).

2.2 Numerical Model and Simulations

To compute the hydrodynamic and the wind-wave fields in the six selected configurations of the Venice Lagoon, we used the two-dimensional (2-D) fully coupled Wind Wave-Tidal Model (WWTM) (Carniello et al., 2005, 2011). The numerical model, coupling a hydrodynamic module and a wind-wave module, describes the hydrodynamic flow field together with the generation and propagation of wind waves using the same computational grid.

The hydrodynamic module uses a semi-implicit staggered finite element method based on Galerkin's approach to solve the 2-D shallow water equations suitably rewritten in order to deal with partially wet and morphologically irregular domains (Defina, 2000; Martini et al., 2004). The bottom shear stress induced by currents, τ_{tc}, is evaluated using the Strickler equation considering the case of a turbulent flow over a rough wall. The hydrodynamic module provides the water levels that are used by the wind-wave module to assess the wave group celerity and the bottom influence on wind-wave propagation.

For the wind-wave module (Carniello et al., 2005, 2011), the wave action conservation equation is parameterized using the zero-order moment of the wave action spectrum in the frequency domain (Holthuijsen et al., 1989). An empirical correlation function relating the peak wave period to the local wind speed and water depth determines the spatial and temporal distribution of the wave period (Young and Verhagen, 1996; Breugem and Holthuijsen, 2007; Carniello et al., 2011). The wind-wave module computes the bottom shear stress induced by wind waves, τ_{ww}, as a function of the maximum horizontal orbital velocity at the bottom, which is related to the significant wave height through the linear theory.

The total bottom shear stress, τ_{wc}, resulting from the combined effect of tidal currents and wind waves, is enhanced beyond the sum of the two contributions, because of the non-linear interaction between the wave and the current boundary layer. In the WWTM this is accounted for by using the empirical formulation suggested by Soulsby (1995, 1997):

$$\tau_{wc} = \tau_{tc} + \tau_{ww}\left[1 + 1.2\left(\frac{\tau_{ww}}{\tau_{ww} + \tau_{tc}}\right)\right] \quad (1)$$

Even if BSSs induced by the tidal currents are typically smaller than those produced by wind waves, they are of fundamental importance in modulating the temporal evolution of the total BSSs and can increase the peak BSS values by up to 30% (Mariotti et al., 2010; D'Alpaos et al., 2013).

The WWTM has been widely tested against field observations not only in the Venice Lagoon (e.g., Carniello et al., 2005, 2011; Tognin et al., 2022) but also in other shallow microtidal environments worldwide, for example in the back-barrier lagoons of the Virginia Coast Reserve (Mariotti et al., 2010) and the Cádiz Bay (Zarzuelo et al., 2018, 2019).

We applied the numerical model to the six computational domains representing the Venice Lagoon and a portion of the Adriatic Sea in front of it in order to perform one-year-long simulations (Figure S1). The boundary conditions of the model are the hourly tidal levels measured at the Consiglio Nazionale delle Ricerche (CNR) Oceanographic Platform, located in the Adriatic Sea offshore of the lagoon, and wind velocities and directions recorded at the Chioggia anemometric station, for which a quite long data set was available (Figure 1a). We forced the model with the time series recorded in 2005, being the probability distribution of wind speeds in 2005 the closest to the mean annual probability distribution in the period 2000-2020 and therefore a representative year for the wind characteristics in the Venice Lagoon (Figure 1b). By considering the same wind and tidal forcing for each historical configuration of the Venice Lagoon, we isolate the effects of the lagoon morphology on the wind-wave fields and on the hydrodynamics.

2.3 Peak Over Threshold Analysis of BSS

The morphodynamic evolution of tidal environments is controlled by the complex interaction among hydrodynamic, biologic and geomorphologic processes, which include both deterministic and stochastic components. As an example, it was shown that sediment transport dynamics in the Venice Lagoon is mostly linked to some limited and severe events induced by wind waves (Carniello et al., 2011), whose dynamics are markedly stochastic in the present-day configuration of the lagoon (D'Alpaos et al., 2013; Carniello et al., 2016). In this work, at any location within each considered configuration of the Venice Lagoon, we used the peak-over-threshold theory (POT) (Balkema and de Haan, 1974) to analyze the temporal and spatial evolution of the total BSS, τ_{wc}. The threshold value of the BSS, τ_c, was set equal to 0.4 Pa (Amos et al., 2004). The POT method allowed us to identify:

1. the interarrival time of over-threshold events, defined as the time between two consecutive upcrossings of the threshold;
2. the duration of over-threshold events, that is the time elapsed between any upcrossing and the subsequent downcrossing of the threshold;
3. its intensity, calculated as the largest exceedance of the threshold in the time elapsed between an upcrossing and the following downcrossing.

Once the probability density functions and the corresponding moments of these variables were defined, a statistical analysis was performed for each location in all the considered configurations of the Venice Lagoon, in order to provide an accurate description of the BSS evolution through the last four centuries. This enabled us to highlight the feedback between morphology and resuspension events over long-term time scales.

We performed the non-parametric Kolmogorov-Smirnov (KS) goodness of fit test to verify the hypothesis that the interarrival time of over-threshold events is an exponentially distributed random variable. The interarrival probability distribution plays an important role because, if interarrival times between subsequent exceedances of the threshold τ_c are independent and exponentially distributed random variables, the mechanics of erosion events can be mathematically described as a 1-D marked Poisson process, characterized by a vector of random marks (intensity and duration of each over-threshold event) associated to a sequence of random events along the time axis. Memorylessness is one of the most interesting mathematical features of Poisson processes since it allows one to set the probability of observing a certain number of events in a pre-established time interval dependent only on its duration, regardless of its position along the time series. Therefore, the description of over-threshold BSS events as a Poisson process will allow one to immediately identify the probabilities of observing a certain number of resuspension events in a year or during a season, because all the sources of stochasticity in the physical drivers are described by a single parameter (i.e. the mean frequency of the process). This suggests the possibility of setting up a synthetic theoretical framework to model the wave-induced events through the use of Monte-Carlo realizations, bearing important consequences for the long-term evolution of tidal landscapes.

3 Results and Discussion

We analyzed the time series of computed total BSSs, τ_{wc}, on the basis of a POT method, in order to provide a statistical characterization of wave-induced erosion events. For all the six historical configurations of the Venice Lagoon, following the approach and the sensitivity analysis suggested by D'Alpaos et al. (2013), we set the critical shear stress, τ_c, equal to 0.4 Pa (Amos et al., 2004) thus neglecting possible effects related to modifications in the bed composition. In order to eliminate spurious upcrossing and downcrossing of the prescribed threshold, the time series of BSSs were previously processed by applying a moving average filter. This low-pass filter with a time window of 6 hours removes short-term fluctuations, preserving the modulation given by the semidiurnal tidal oscillation. Thanks to this procedure, over-threshold events satisfy the independence assumption required by the statistical analysis applied.

At any node of the computational grids reproducing the selected configurations of the Venice Lagoon, the probability distributions of interarrival time, peak excess and duration of over-threshold erosion events are compared with an exponential distribution performing the KS test with a significance level $\alpha = 0.05$. Figure 3 shows the results of the KS test spatially distributed over the considered domains. In particular, we distinguished:

1. the dark blue area, where the KS test is not verified for the interarrival time, i.e. wave-induced erosion events can not be described as a Poisson process;

2. the red area, where the KS test is verified for all the three considered stochastic variables, namely interarrival times, intensity, and duration, i.e. wave-induced erosion events are indeed a marked Poisson process where its markers, intensity and duration, are exponentially distributed random variables;

3. the yellow area, where the KS test is verified for the interarrival time but it is not verified for the intensity and/or duration, i.e. wave-induced erosion events are a marked Poisson process but at least one between intensity and duration is not an exponentially distributed random variable.

The mean interarrival times (Figure 4), mean peak excesses (Figure 5) and mean durations of over-threshold erosion events (Figure 6) in the six selected configurations of the Venice Lagoon are shown in every location where the KS test is satisfied for interarrival times (Figure 3), and, thus, erosion events, can be described as a Poisson process.

Wind-wave generation is determined by energy transfer from the wind to the water surface and, thus, it clearly depends on wind characteristics, namely wind intensity and duration, as well as on fetch length and water depth (Fagherazzi et al., 2006; Fagherazzi and Wiberg, 2009). As a consequence, the spatial distribution and morphological characteristics of channels, tidal flats, and, more importantly, salt marshes and islands strongly influence the response of a shallow tidal basin to wind forcing and the resulting distribution of BSSs (Fagherazzi et al., 2006; Defina et al., 2007). Large portions in the ancient configurations of the lagoon were occupied by salt-marsh areas, continuously interrupting the fetch and thus reducing the exceedances of the critical threshold. As a result, in the four more ancient configurations the characteristics of erosion events globally display a more complex spatial pattern, which conversely tends to be more uniform in the recent most configurations, due to the reduction in salt-marsh areas, to the increase in fetch length, and to the deepening of tidal flats.

In all the selected configurations, salt marshes and tidal channel networks mostly represent the portion of the lagoon where wave-induced erosion events cannot be modeled as a Poisson process (dark blue area in Figure 3). Over salt-marsh platforms almost no exceedances of the prescribed threshold, τ_c, tend to occur (Figure S2) because of the low water depth that prevents the formation of significant waves (e.g., Möller et al., 1999). May we add that colonization of the salt-marsh surface by halophytic vegetation almost completely prevents any vertical erosion (Christiansen et al., 2000; Temmerman et al., 2005). On the contrary, exceedances of the threshold can be detected along the channel network and at the three inlets (Figure S2), but these are mostly associated with shear stresses produced by tidal currents, especially after the construction of the jetties at the

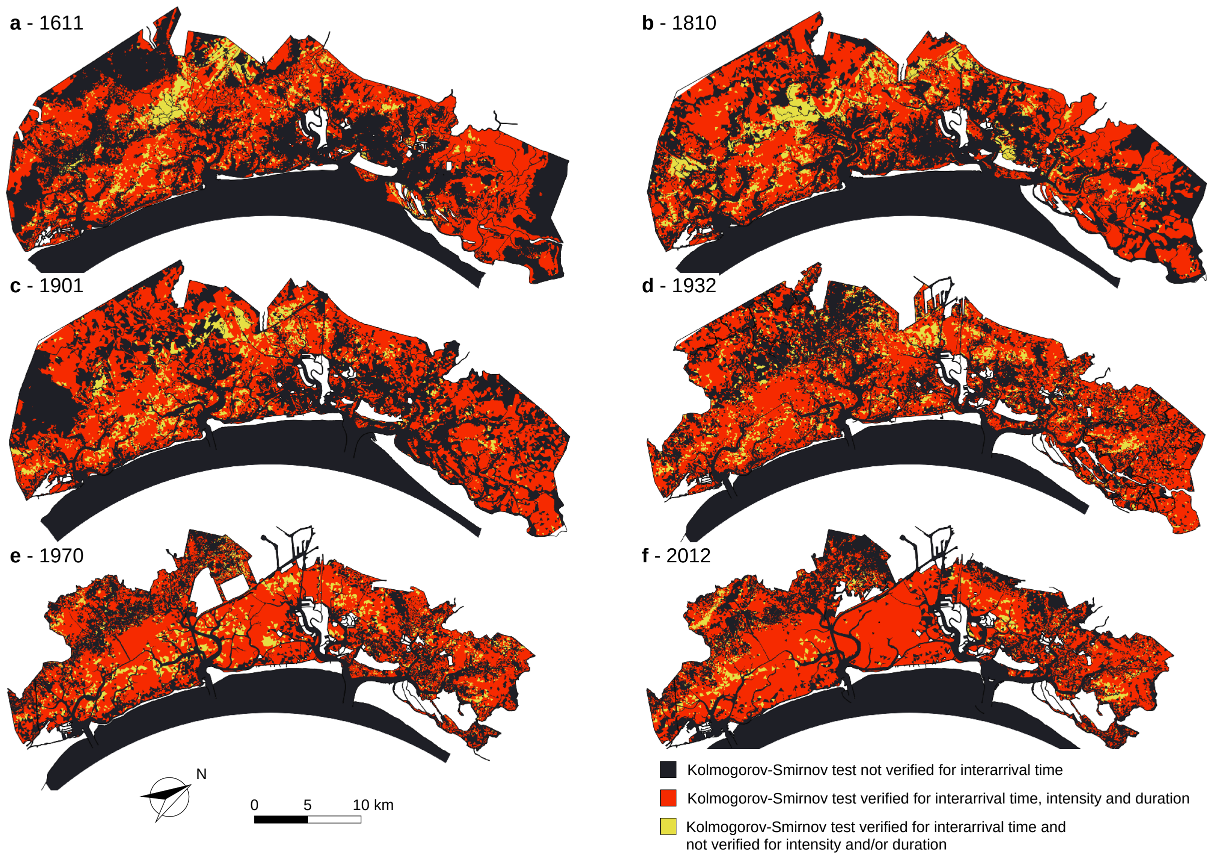

Figure 3. Kolmogorov-Smirnov test for over-threshold erosion events. Spatial distribution of Kolmogorov-Smirnov (KS) test at significance level ($\alpha = 0.05$) for the six different configurations of the Venice Lagoon: 1611 (**a**), 1810 (**b**), 1901 (**c**), 1932 (**d**), 1970 (**e**), and 2012 (**f**). In the maps we can distinguish areas where the KS test is: not verified (dark blue); verified for all the considered stochastic variables (interarrival time, intensity over the threshold and duration) (red); verified for the interarrival time and not for intensity and/or duration (yellow).

inlets. Consequently, at these points the KS test is not satisfied and erosion events cannot be modeled as a Poisson process because of the strictly deterministic nature of tide-induced shear stress.

Figure 7 shows the time series and the probability distribution at the SM station in the Malamocco inlet (see Figure 1a for the location). In the 1611 and 1810 simulations, in the absence of jetties at the inlets, the BSS was very small, so that the number of exceedances of the threshold was too low to be representative (Figure 7a,b). After the construction of the jetties at the Malamocco inlet in 1872, erosion mechanics abruptly changed: BSS considerably increased but it was driven by tidal forcing and, thus, interarrival times were not exponentially distributed, since the erosion threshold was exceeded on average once per day because of tidal fluxes (Figure 7c-f). The BSS analysis at the SL station in the Lido inlet, where the construction of the jetties ended in 1892, provides analogous results (Figure S3). Whereas, at the SC station in the Chioggia inlet, BSS still

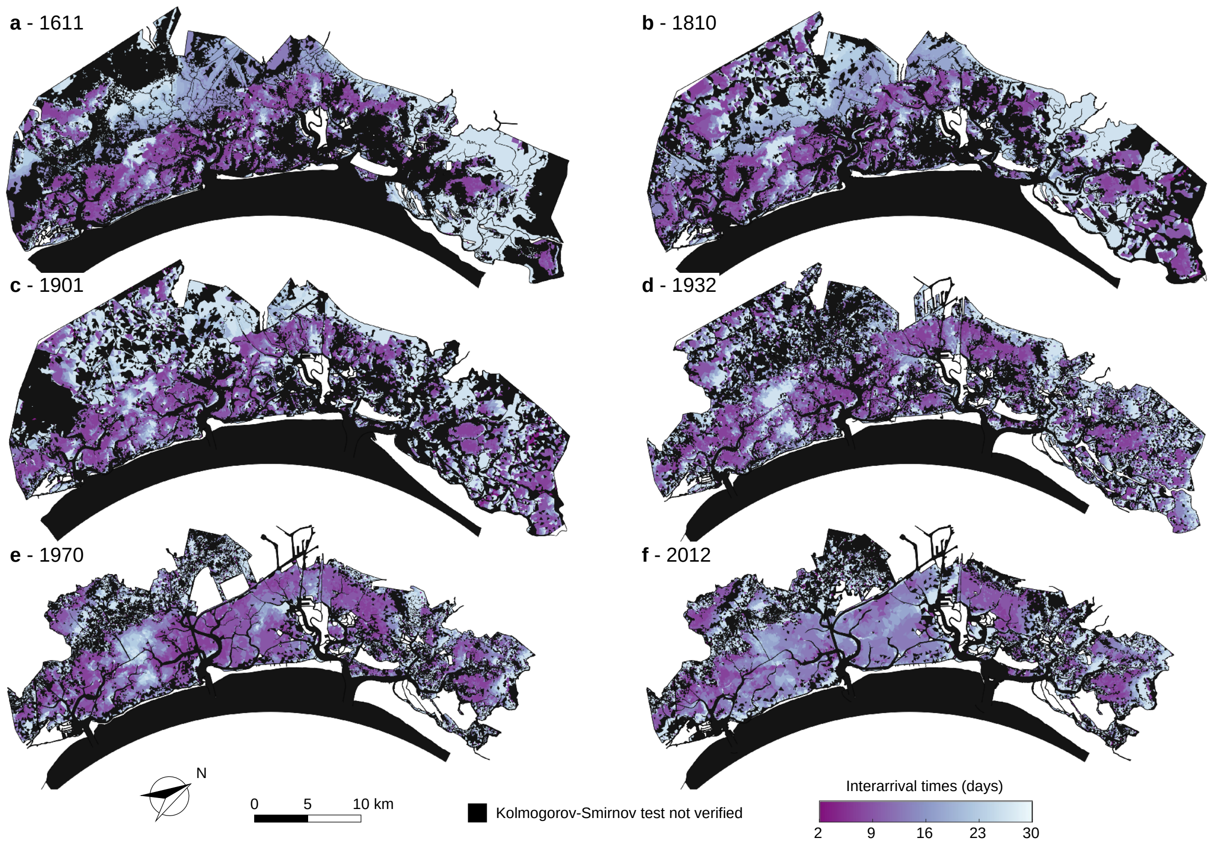

Figure 4. Mean interarrival time of over-threshold erosion events. Spatial distribution of mean interarrival times of over-threshold exceedances at sites where bed shear stress can be modeled as a marked Poisson process, as confirmed by the KS test ($\alpha = 0.05$) for the six different configurations of the Venice Lagoon: 1611 (**a**), 1810 (**b**), 1901 (**c**), 1932 (**d**), 1970 (**e**), and 2012 (**f**).

does not systematically exceed the threshold also in the 1901 configuration, since the construction of the jetties at the Chioggia inlet took place between 1930 and 1934 (D'Alpaos, 2010b) (Figure S4).

The KS test is verified over subtidal platforms and tidal flats, where current-induced BSSs are typically below the critical value, but wave-induced BSSs mainly contribute to the total BSS. Locations where interarrival time, duration and intensity follow an exponential distribution (see red areas in Figure 3) remain the vast majority of the tidal basin in all the configurations. As a result, a synthetic framework that models erosion as a Poisson process is deemed to be suitable for wide tidal-flat areas.

Almost in all configurations, large interarrival times (Figure 4) are essentially found in sheltered areas, where only particularly intense events are able to generate BSSs large enough to exceed τ_c. A clear example is provided by the area protected by marsh platforms and by the mainland in the northeastern and in the western portion of the lagoon, sheltered from the north-easterly Bora wind, which is the main morphologically significant wind in the Venice Lagoon (Figure 1b). This pattern becomes even more evident in the configurations of 1611, 1810, and 1901 where portions of the lagoon occupied by salt marshes are

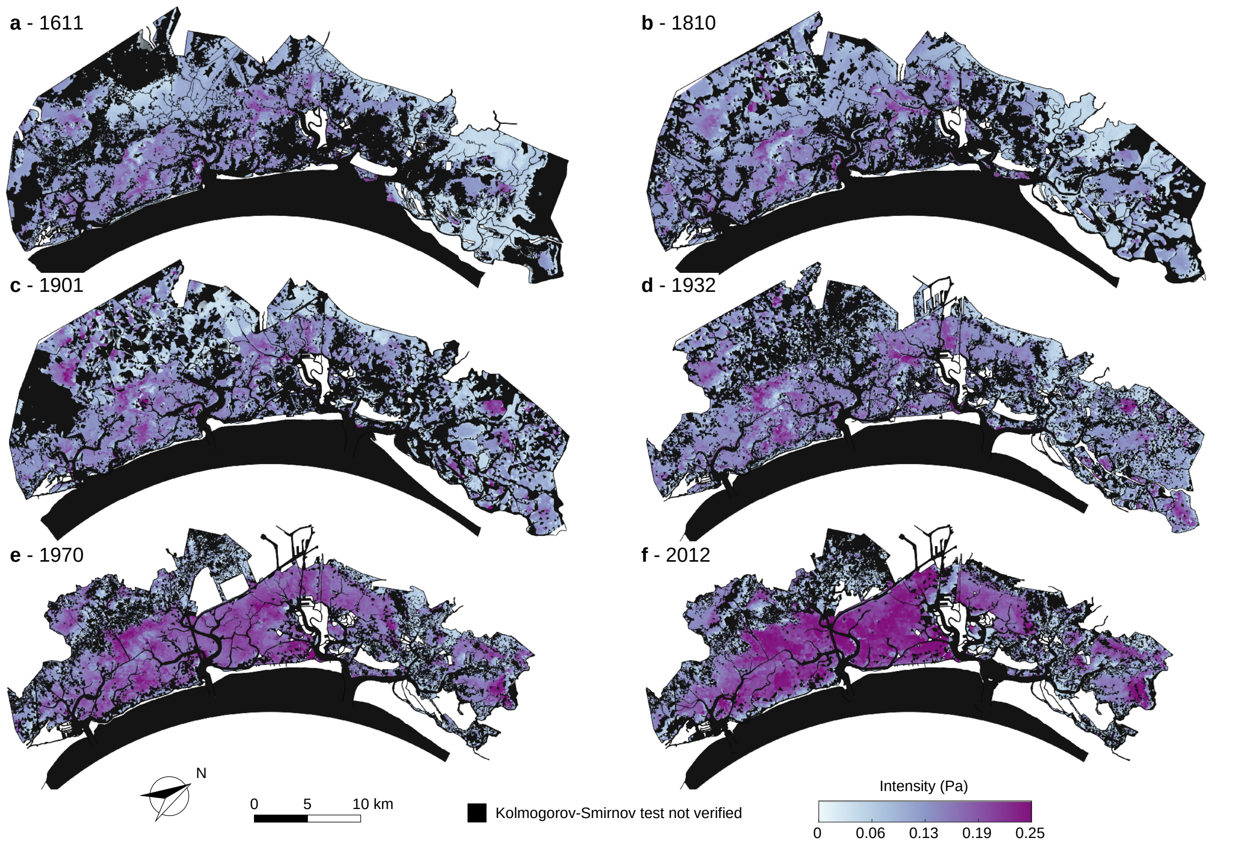

Figure 5. Mean intensity of over-threshold erosion events. Spatial distribution of mean intensity of peak excesses of over-threshold exceedances at sites where bed shear stress can be modeled as a marked Poisson process, as confirmed by the KS test ($\alpha = 0.05$) for the six different configurations of the Venice Lagoon: 1611 (**a**), 1810 (**b**), 1901 (**c**), 1932 (**d**), 1970 (**e**), and 2012 (**f**).

wider than in the more recent configurations and display interarrival times longer than 30 days. Large interarrival times can also be observed close to the three inlets where the water depth is such that only during intense events the bottom can be affected by wave oscillations and the total BSSs can exceed the threshold. Globally speaking, in the four oldest configurations we found relatively short (about 5 days) interarrival times spread all around the lagoon, while the present configuration, characterized by a more uniform and larger water depth (in some areas deeper than 1.5 m), displays longer interarrival times, e.g., between 10 and 15 days for the tidal flats located in the central-southern portion of the lagoon (Figure 4 and S5a). This is mainly due to the relationship existing between τ_{ww} and water depth that, for a prescribed wind velocity, decreases as the water depth increases (Defina et al., 2007). Indeed, in the historical configurations large areas occupied by tidal flats are characterized by lower water depth (≤ 0.5 m), and, as a result, τ_{ww} is higher also for weak wind speeds, thus increasing the number of exceedances of the threshold.

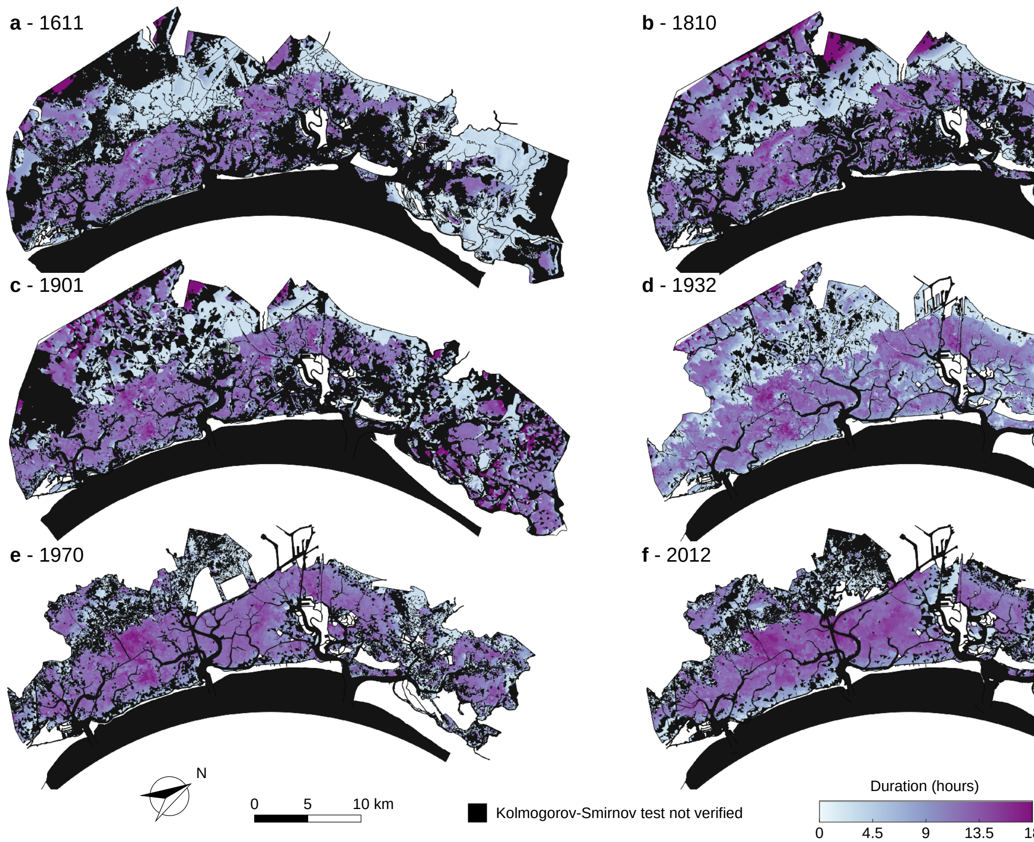

Figure 6. Mean durations of over-threshold erosion events. Spatial distribution of mean durations of over-threshold exceedances at sites where bed shear stress can be modeled as a marked Poisson process, as confirmed by the KS test ($\alpha = 0.05$) for the six different configurations of the Venice Lagoon: 1611 (**a**), 1810 (**b**), 1901 (**c**), 1932 (**d**), 1970 (**e**), and 2012 (**f**).

Figure 8a shows the probability distributions of the interarrival times for station S1, located on a relatively shallow tidal flat in the northern lagoon named "Palude Maggiore" (see Figure 1a), which maintained the same morphological features through the last four centuries. At this point, as in most areas of the lagoon, the mean interarrival time $\overline{\lambda}_t$ between two subsequent over-threshold events increases through time. On the contrary, the tidal flat in the watershed divide area between the Chioggia and the Malamocco inlets, named "Fondo dei Sette Morti" (see point S2 in Figure 1a), shows a reverse trend: the interarrival times decrease in time from 1611 to nowadays (i.e. wave-induced erosion events are more frequent, Figure 8d). Although the almost constant, relatively deep bottom elevation that characterized this area through centuries (Carniello et al., 2009; D'Alpaos, 2010b) prevents the exceedance of the threshold τ_c during less intense erosion events, the generalized deepening experienced by the surrounding portion of the lagoon in the most recent configurations promotes more frequent and less intense events within this area and, therefore, a decrease of the interarrival times.

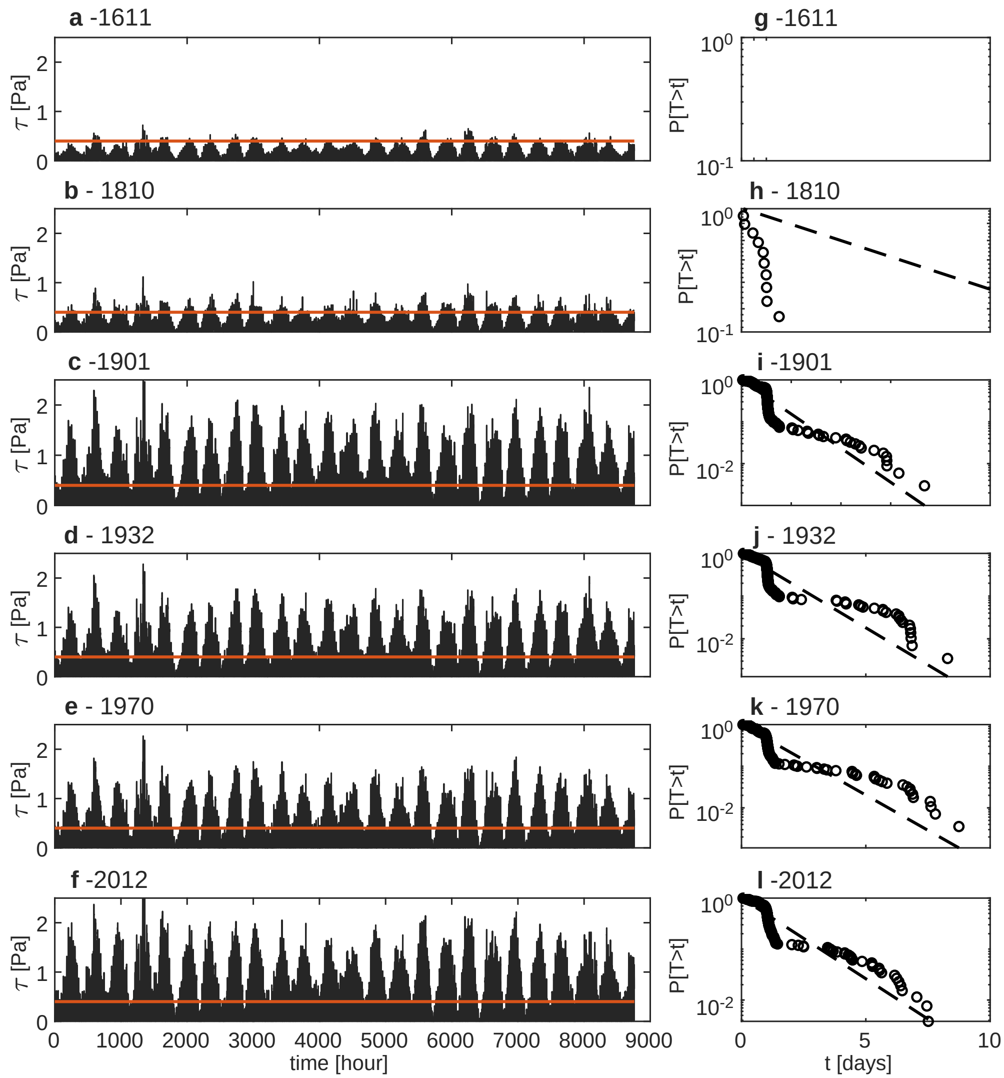

Figure 7. Over-threshold BSS events at the Malamocco inlet. Statistical analysis at SM station in the Malamocco inlet: time series of the computed BSS (**a-f**); probability distributions of the interarrival times (circles) and exponential distributions (dashed lines) (**g-l**).

The over-threshold peak intensities generally strongly increased during the last four centuries (Figure 5 and S5b). For all the selected configurations, intensities are lower in the more pristine northern part of the lagoon, which is sheltered from the dominant Bora wind by the mainland and by preserved salt-marsh areas, interrupting the fetch. Whereas the central and southern portions of the lagoon are characterized by much larger intensity values, which more rapidly increased over the last

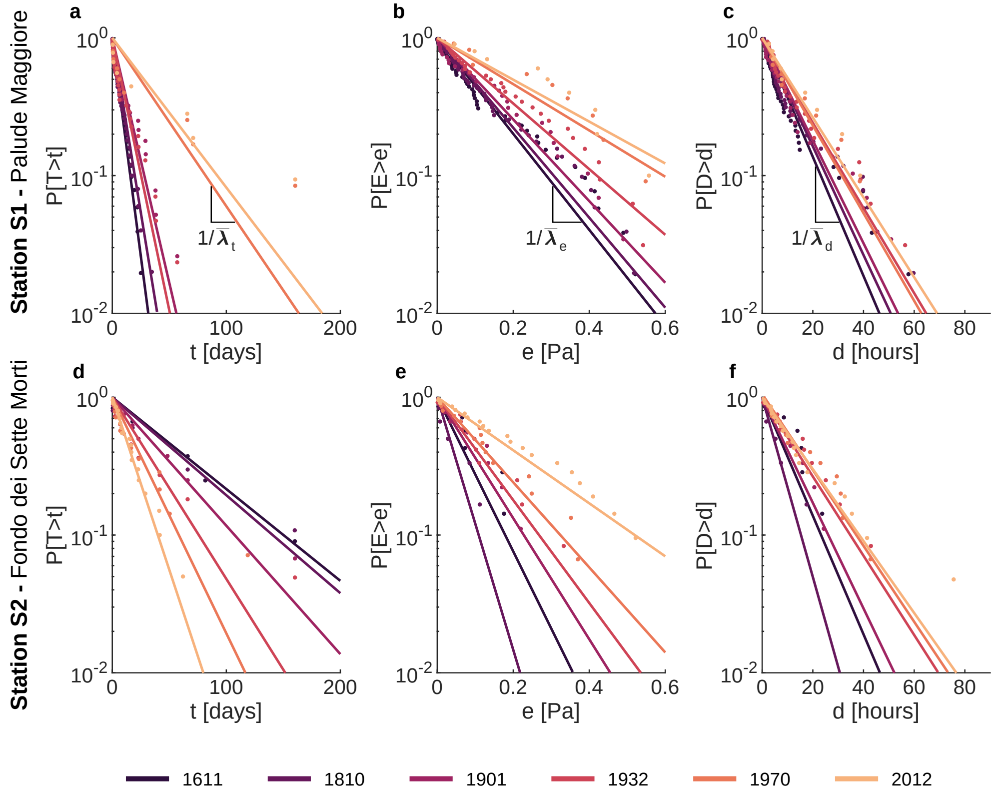

Figure 8. Over-threshold erosion events at stations S1 and S2. Statistical characterizations of over-threshold events at two stations S1 "Palude Maggiore" and S2 "Fondo dei Sette Morti" (see Figure 1a for locations) in the six configurations of the Venice Lagoon. Probability distributions of (**a-b**) interarrival times, t; (**c-d**) intensities of peak excesses of over-threshold exceedances, e; and (**e-f**) durations of over-threshold event, d. $\overline{\lambda}_t$ mean interarrival time, $\overline{\lambda}_e$ mean peak excess intensity, and $\overline{\lambda}_d$ mean duration.

few decades. In particular, in the central part of the lagoon the mean intensities increased from around 0.13 Pa to 0.25 Pa above the threshold, due to the flattening and deepening of this area. A quite similar situation characterizes also the southern part of the Venice Lagoon, between the Malamocco and Chioggia inlets.

For all the configurations investigated, the durations of over-threshold events (Figure 6 and S5c), likewise intensities, present much lower values in the areas sheltered by salt marshes (i.e. the northern lagoon and the western portion of the southern lagoon) than in the fetch-unlimited central-southern portion of the lagoon. In the latter area, indeed, over-threshold events last more than 15 hours, compared to a duration of about 5 hours in the more sheltered areas. The increase of peak intensities and durations of erosion events over time is also clearly shown by the probability distributions computed at points S1 and S2 (Figure 8).

The larger over-threshold peak intensities, as well as the longer durations characterizing the central-southern portion of the lagoon and increasing from the past to the present, are in agreement with recent observations highlighting a critical erosive trend for the tidal flats and subtidal platforms in this area (Carniello et al., 2009; Molinaroli et al., 2009; D'Alpaos, 2010b; Defendi et al., 2010; Sarretta et al., 2010).

To investigate the relationship among the three random variables, the temporal cross-correlation is computed for each location and for all six configurations (Figures S6, S7 and S8). In particular, the temporal cross-correlation between intensity of peak excesses and duration of over-threshold exceedances display values very close to 1 for all the lagoon morphologies, thus suggesting a pseudo-deterministic link between peak intensities and the corresponding durations (Figure S6 and S9a). On the contrary, almost no correlation exists between durations and interarrival times (Figure S7 and S9b), as well as between intensities and interarrival times (Figure S8 and S9c). These results, in line with the temporal cross-correlation obtained for the statistical analysis of suspended sediment concentration for the present lagoon by Carniello et al. (2016), suggest that resuspension events can be modeled as a 3-D Poisson process in which the marks (duration and intensity) are mutually dependent but independent from the interarrival time between two subsequent over-threshold events.

In order to provide a more quantitative estimation of the spatial heterogeneity of interarrival times, duration and intensities of the critical BSS exceedances, we computed the "erosion work" (geomorphic work *sensu* Wolman and Miller (1960), see also Mariotti and Fagherazzi (2013)), which represents the amount of sediment actually resuspended during a selected time interval. The erosion work $[E_w^*]$ experienced by a single point during the time interval $(t_2 - t_1)$ can be computed as:

$$[E_w^*] = \int_{t_1}^{t_2} \frac{e}{\rho_b} \left(\frac{\tau_{wc} - \tau_c}{\tau_c} \right) \mathrm{d}t. \tag{2}$$

where e is the value of the erosion coefficient which depends on the sediment properties and $\rho_b = \rho_s(1-n)$ is the sediment bulk density, being n the porosity. We set e equal to $5 \cdot 10^{-5}$ kg m^{-2} s^{-1}, as suggested for sand-mud mixtures (van Ledden et al., 2004; Le Hir et al., 2007) and in agreement with Carniello et al. (2012), $\rho_s = 2650$ kg m^{-3} and $n = 0.4$.

Using the mean values of the stochastic variables considered herein (i.e. interarrival time, intensity and duration), once verified they can be modeled as a Poisson process, we can simplify Eq. 2 as follows:

$$[E_w] = \frac{e}{\rho_b} \left(\frac{\tau_{wc} - \tau_c}{\tau_c} \right) (t_2 - t_1) \tag{3}$$

where we assume $(t_2 - t_1)$ to be the mean duration of over-threshold events and $(\tau_{wc} - \tau_c)$ their mean intensity. In order to estimate the erosion work for one year, E_w, we multiplied the result obtained with the Eq. 3 for the number of events, computed as 365 (days per year) divided by the mean interarrival time at each point within the lagoon. Instead, using the complete formulation in Eq. 2, the erosion work over one year, E_w^*, can be simply computed simply by extending the integration period to the entire year.

Figure 9 provides the spatial distribution of the annual erosion work, E_w, for the six configurations of the Venice Lagoon. We computed the erosion work also according to Eq. 2, in order to compare differences between the complete formulation based on the computed BSS time records and the synthetic approach exploiting the possibility of describing resuspension events as marked Poisson processes (Figure S10). The erosion work computed following the two approaches is quite similar, as shown by the map of the relative error (Figure S11) and by the computed values of the spatially averaged relative error which varies between 10% and 14% considering all the analyzed configurations of the lagoon (Table 1). Such an agreement between the two estimates of the erosion work supports the validity of the provided statistical characterization of resuspension events.

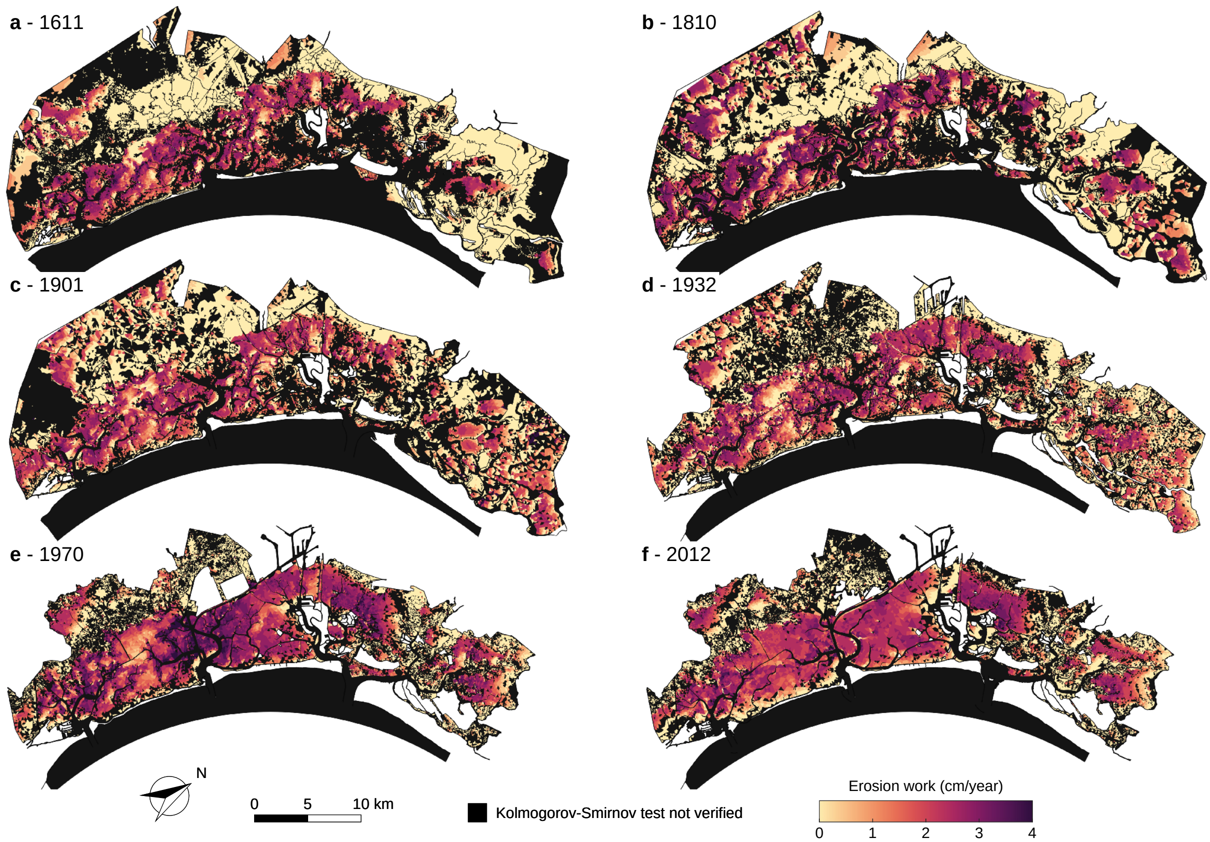

Figure 9. Erosion work. Spatial distribution of erosion work for the six different configurations of the Venice Lagoon: 1611 (**a**), 1810 (**b**), 1901 (**c**), 1932 (**d**), 1970 (**e**), and 2012 (**f**). Black identifies sites where the bottom shear stress cannot be modeled as a marked Poisson process (i.e. the KS test is not verified for the interarrival time).

Focusing in particular on the central-southern lagoon, the erosion work is almost constant between 1611 and 1932, it reaches its maximum in 1970 and then it decreases in the present configuration (Figure 9). The four most ancient configurations (i.e. 1611, 1810, 1901 and 1932) display a more complex spatial pattern of the computed erosion work because of the wider presence of salt marshes and islands distributed throughout the basin and because of the shallower and more irregular bathymetry characterizing the tidal flats. This morphology is such that the fetch is continuously interrupted and wind waves are prevented from fully developing while generating and propagating over areas whose bathymetry is continuously varying. Interestingly, even if the present configuration of the lagoon displays larger mean intensities and longer mean durations than in 1970 (see Figure 5 and Figure 6), the combination with generally longer mean interarrival times (Figure 4) affects the erosion work. Indeed, the erosion work is maximum in the 1970 configuration when it reaches a peak of more than 4.0 cm/year. This promoted an intense and uniform erosion of the lagoon, thus leading to the present morphology and bathymetry characterized by less complex erosion patterns and a roughly constant erosion work on the tidal flats in the central-southern lagoon of about 2.5 cm/year. Our results quantitatively support previous studies (Carniello et al., 2009; Molinaroli et al., 2009) that identified two different evolutionary trends in the northern lagoon and in the central-southern part, the northern lagoon displaying, on average, much lower erosion rates.

Table 1. Spatially averaged relative error between erosion work computed with Eq. 2 and 3

Configuration	r_e [-]
1611	0.140
1810	0.108
1901	0.135
1932	0.131
1970	0.133
2012	0.112

4 Conclusions

Our results provide a statistical characterization of sediment erosion in shallow tidal environments, aimed at testing the possibility to describe erosion dynamics as a Poisson process in a synthetic modeling framework able to reproduce the long-term evolution of shallow tidal environments. The approach is applied to the specific case of the Venice Lagoon, for which six morphological configurations along the last four centuries are available.

In the present study, we applied the extensively calibrated and tested Wind Wave-Tidal Model to the six historical configurations of the Venice Lagoon, in order to perform a spatially-explicit analysis of the BSS time series under the same wind and water level forcing. We analyzed the computed BSS temporal evolution following the peak-over-threshold theory. We verified whether wind-wave erosion events could be modeled as a marked Poisson process by performing the non-parametric Kolmogorov-Smirnov goodness of fit test to confirm the hypothesis that the interarrival time of over-threshold BSS events together with their durations and intensities are exponentially distributed random variables.

Statistical analyses of the wave-driven erosion processes suggest that interarrival times between two consecutive over-threshold events, their durations and intensities can be described as exponentially distributed random variables over wide areas in all the selected configurations of the Venice Lagoon. As a consequence, the wave-induced erosion can be represented by a marked Poisson process through centuries.

Furthermore, we observed that durations and intensities of over-threshold BSS exceedances are highly correlated, while almost no correlation exists between duration and interarrival time, as well as between intensity and interarrival time. These observations indicate that a 3-D Poisson process, in which the marks (duration and intensity of the over-threshold events) are mutually dependent but independent from the interarrival time, provides a suitable description of the wave-induced erosion processes.

Moreover, we showed that in the last four centuries the interarrival times of erosion events generally increased everywhere within the lagoon, as well as their intensities and durations, thus leading to less frequent but more intense wave-induced erosion events. These modifications in the bottom shear stress field are generated by, but at the same time they are also responsible for, the morphological modifications of the Venice Lagoon, in particular the generalized deepening of tidal flats and reduction of salt-marsh area. Only in the “Fondo dei Sette Morti", located close to the watershed divide between the Malamocco and the Chioggia inlets, interarrival times decrease in the last four centuries. Such an opposite trend is associated with the relatively deep and constant bottom elevation characterizing this area combined with the generalized deepening experienced by the surrounding areas that allows more frequent events reaching the “Fondo dei Sette Morti".

The erosion work, computed as a combination of interarrival times, durations and intensities, remained almost constant and characterized by an irregular spatial pattern until the beginning of the twentieth century, when it rapidly increased reaching a peak in 1970. In the last few decades, the erosion work decreased, presenting a more uniform pattern and suggesting that the quite intense erosive trend the Venice Lagoon has been experiencing since the beginning of the last century is, at present, slowing down as a consequence of the generalized deepening and flattening of the lagoonal bed. Owing to the choice of forcing the domain with the same conditions, these changes in the erosive trend are, in fact, only due to morphological modifications experienced by the tidal basin.

The present findings, together with the statistical characterization of suspended sediment dynamics (Tognin et al., Companion paper), represent a step towards the set up of a synthetic, statistically-based framework which can be used to model the long-term morphodynamic evolution of shallow tidal systems through the use of independent Monte Carlo realizations, thus possibly exploring a large set of equally likely lagoonal configurations.

Data availability. All data presented in this study and used for the analysis of the bottom shear stress are available at https://researchdata.cab.unipd.it/id/eprint/728 (10.25430/researchdata.cab.unipd.it.00000728)

Author contributions. Conceptualization: Andrea D’Alpaos, Andrea Rinaldo, Luca Carniello, Davide Tognin;
Methodology: Davide Tognin, Andrea D’Alpaos, Luca Carniello;
Formal analysis and investigation: Davide Tognin, Laura Tommasini;
Figures: Davide Tognin;
Writing - original draft preparation: Davide Tognin, Laura Tommasini;
Writing - review and editing: all authors;
Funding acquisition: Andrea D’Alpaos, Luca Carniello;
Resources: Andrea D’Alpaos, Luca Carniello, Luigi D’Alpaos, Andrea Rinaldo;
Supervision: Andrea D’Alpaos, Luca Carniello.

Competing interests. The authors declare no competing interests.

Acknowledgements. This scientific activity was partially performed as part of the Research Programme Venezia2021, with contributions from the Provveditorato for the Public Works of Veneto, Trentino Alto Adige and Friuli Venezia Giulia, provided through the concessionary of State Consorzio Venezia Nuova and coordinated by CORILA, Research Line 3.2 (PI A.D.), by the 2019 University of Padova project (BIRD199419) ‘Tidal network ontogeny and evolution: a comprehensive approach based on laboratory experiments with ancillary numerical modelling and field measurements’ (PI L.C.), and by University of Padova SID2021 project, ‘Unraveling Carbon Sequestration Potential by Salt-Marsh Ecosystems’ (P.I. A. D.).

References

Amos, C. L., Bergamasco, A., Umgiesser, G., Cappucci, S., Cloutier, D., Denat, L., Flindt, M., Bonardi, M., and Cristante, S.: The stability of tidal flats in Venice Lagoon - The results of in-situ measurements using two benthic, annular flumes, Journal of Marine Systems, https://doi.org/10.1016/j.jmarsys.2004.05.013, 2004.

Balkema, A. A. and de Haan, L.: Residual Life Time at Great Age, The Annals of Probability, https://doi.org/10.1214/aop/1176996548, 1974.

Belliard, J.-P., Silinski, A., Meire, D., Kolokythas, G., Levy, Y., Van Braeckel, A., Bouma, T. J., and Temmerman, S.: High-resolution bed level changes in relation to tidal and wave forcing on a narrow fringing macrotidal flat: Bridging intra-tidal, daily and seasonal sediment dynamics, Marine Geology, 412, 123–138, https://doi.org/10.1016/j.margeo.2019.03.001, 2019.

Bendoni, M., Mel, R. A., Solari, L., Lanzoni, S., Francalanci, S., and Oumeraci, H.: Insights into lateral marsh retreat mechanism through localized field measurements, Water Resources Research, https://doi.org/10.1002/2015WR017966, 2016.

Botter, G., Porporato, A., Rodriguez-Iturbe, I., and Rinaldo, A.: Basin-scale soil moisture dynamics and the probabilistic characterization of carrier hydrologic flows: Slow, leaching-prone components of the hydrologic response, Water Resources Research, https://doi.org/10.1029/2006WR005043, 2007.

Breugem, W. A. and Holthuijsen, L. H.: Generalized Shallow Water Wave Growth from Lake George, Journal of Waterway, Port, Coastal, and Ocean Engineering, https://doi.org/10.1061/(asce)0733-950x(2007)133:3(173), 2007.

Carbognin, L., Teatini, P., and Tosi, L.: Eustacy and land subsidence in the Venice Lagoon at the beginning of the new millennium, Journal of Marine Systems, https://doi.org/10.1016/j.jmarsys.2004.05.021, 2004.

Carniello, L., Defina, A., Fagherazzi, S., and D'Alpaos, L.: A combined wind wave-tidal model for the Venice lagoon, Italy, Journal of Geophysical Research: Earth Surface, 110, 1–15, https://doi.org/10.1029/2004JF000232, 2005.

Carniello, L., Defina, A., and D'Alpaos, L.: Morphological evolution of the Venice lagoon: Evidence from the past and trend for the future, Journal of Geophysical Research, 114, F04 002, https://doi.org/10.1029/2008JF001157, 2009.

Carniello, L., D'Alpaos, A., and Defina, A.: Modeling wind waves and tidal flows in shallow micro-tidal basins, Estuarine, Coastal and Shelf Science, 92, 263–276, https://doi.org/10.1016/j.ecss.2011.01.001, 2011.

Carniello, L., Defina, A., and D'Alpaos, L.: Modeling sand-mud transport induced by tidal currents and wind waves in shallow microtidal basins: Application to the Venice Lagoon (Italy), Estuarine, Coastal and Shelf Science, 102-103, 105–115, https://doi.org/10.1016/j.ecss.2012.03.016, 2012.

Carniello, L., D'Alpaos, A., Botter, G., and Rinaldo, A.: Statistical characterization of spatiotemporal sediment dynamics in the Venice lagoon, Journal of Geophysical Research: Earth Surface, pp. 1049–1064, https://doi.org/10.1002/2015JF003793, 2016.

Carr, J. A., D'Odorico, P., McGlathery, K. J., and Wiberg, P. L.: Stability and bistability of seagrass ecosystems in shallow coastal lagoons: Role of feedbacks with sediment resuspension and light attenuation, Journal of Geophysical Research: Biogeosciences, 115, https://doi.org/10.1029/2009JG001103, 2010.

Chen, X., Zhang, C., Zhou, Z., Gong, Z., Zhou, J. J., Tao, J. F., Paterson, D. M., and Feng, Q.: Stabilizing Effects of Bacterial Biofilms: EPS Penetration and Redistribution of Bed Stability Down the Sediment Profile, Journal of Geophysical Research: Biogeosciences, https://doi.org/10.1002/2017JG004050, 2017.

Christiansen, T., Wiberg, P. L., and Milligan, T. G.: Flow and Sediment Transport on a Tidal Salt Marsh Surface, Estuarine, Coastal and Shelf Science, 50, 315–331, https://doi.org/10.1006/ecss.2000.0548, 2000.

D'Alpaos, A., Da Lio, C., and Marani, M.: Biogeomorphology of tidal landforms : physical and biological processes shaping the tidal landscape, Ecohydrology, 5, 550–562, https://doi.org/10.1002/eco.279, 2012.

D'Alpaos, A., Carniello, L., and Rinaldo, A.: Statistical mechanics of wind wave-induced erosion in shallow tidal basins: Inferences from the Venice Lagoon, Geophysical Research Letters, https://doi.org/10.1002/grl.50666, 2013.

D'Alpaos, L.: Fatti e misfatti di idraulica lagunare. La laguna di Venezia dalla diversione dei fiumi alle nuove opere delle bocche di porto, Istituto Veneto di Scienze, Lettere e Arti, Venice, 2010a.

D'Alpaos, L.: L'evoluzione morfologica della laguna di Venezia attraverso la lettura di alcune mappe storiche e delle sue mappe idrografiche, Istituto Veneto di Scienze, Lettere e Arti, 2010b.

D'Alpaos, L. and Martini, P.: The influence of inlet configuration on sediment loss in the Venice lagoon, in: Flooding and Environmental Challenges for Venice and its Lagoon: State of Knowledge, edited by Fletcher, C. A. and Spencer, T., pp. 419–430, Cambridge University Press, Cambridge, 2005.

Defendi, V., Kovačević, V., Arena, F., and Zaggia, L.: Estimating sediment transport from acoustic measurements in the Venice Lagoon inlets, Continental Shelf Research, 30, 883–893, https://doi.org/10.1016/j.csr.2009.12.004, 2010.

Defina, A.: Two-dimensional shallow flow equations for partially dry areas, Water Resources Research, 36, 3251–3264, https://doi.org/10.1029/2000WR900167, 2000.

Defina, A., Carniello, L., Fagherazzi, S., and D'Alpaos, L.: Self-organization of shallow basins in tidal flats and salt marshes, Journal of Geophysical Research: Earth Surface, 112, 1–11, https://doi.org/10.1029/2006JF000550, 2007.

D'Odorico, P. and Fagherazzi, S.: A probabilistic model of rainfall-triggered shallow landslides in hollows: A long-term analysis, Water Resources Research, https://doi.org/10.1029/2002WR001595, 2003.

Fagherazzi, S. and Wiberg, P. L.: Importance of wind conditions, fetch, and water levels on wave-generated shear stresses in shallow intertidal basins, Journal of Geophysical Research: Earth Surface, https://doi.org/10.1029/2008JF001139, 2009.

Fagherazzi, S., Carniello, L., D'Alpaos, L., and Defina, A.: Critical bifurcation of shallow microtidal landforms in tidal flats and salt marshes, Proceedings of the National Academy of Sciences, 103, 8337–8341, https://doi.org/10.1073/pnas.0508379103, 2006.

Finotello, A., Marani, M., Carniello, L., Pivato, M., Roner, M., Tommasini, L., and D'alpaos, A.: Control of wind-wave power on morphological shape of salt marsh margins, Water Science and Engineering, 13, 45–56, https://doi.org/10.1016/j.wse.2020.03.006, 2020.

Finotello, A., Tognin, D., Carniello, L., Ghinassi, M., Bertuzzo, E., and D'Alpaos, A.: Hydrodynamic feedbacks of salt-marsh loss in shallow microtidal back-barrier systems, Earth and Space Science Open Archive, p. 32, https://doi.org/10.1002/essoar.10511787.2, 2022.

Ghinassi, M., D'Alpaos, A., Tommasini, L., Brivio, L., Finotello, A., and Stefani, C.: Tidal currents and wind waves controlling sediment distribution in a subtidal point bar of the Venice Lagoon (Italy), Sedimentology, 66, 2926–2949, https://doi.org/https://doi.org/10.1111/sed.12616, 2019.

Goodbred, Steven L., J. and Hine, A. C.: Coastal storm deposition: Salt-marsh response to a severe extratropical storm, March 1993, west-central Florida, Geology, 23, 679–682, https://doi.org/10.1130/0091-7613(1995)023<0679:CSDSMR>2.3.CO;2, 1995.

Green, M. O. and Coco, G.: Review of wave-driven sediment resuspension and transport in estuaries, Reviews of Geophysics, 52, 77–117, https://doi.org/10.1002/2013RG000437, 2014.

Holthuijsen, L. H., Booij, N., and Herbers, T. H. C.: A prediction model for stationary, short-crested waves in shallow water with ambient currents, Coastal Engineering, 13, 23–54, https://doi.org/https://doi.org/10.1016/0378-3839(89)90031-8, 1989.

Hu, Z., Yao, P., van der Wal, D., and Bouma, T. J.: Patterns and drivers of daily bed-level dynamics on two tidal flats with contrasting wave exposure, Scientific Reports, 7, 7088, https://doi.org/10.1038/s41598-017-07515-y, 2017.

Lawson, S. E., Wiberg, P. L., McGlathery, K. J., and Fugate, D. C.: Wind-driven sediment suspension controls light availability in a shallow coastal lagoon, Estuaries and Coasts, 30, 102–112, https://doi.org/10.1007/BF02782971, 2007.

Le Hir, P., Monbet, Y., and Orvain, F.: Sediment erodability in sediment transport modelling: Can we account for biota effects?, Continental Shelf Research, 27, 1116–1142, https://doi.org/10.1016/j.csr.2005.11.016, 2007.

Leonardi, N., Ganju, N. K., and Fagherazzi, S.: A linear relationship between wave power and erosion determines salt-marsh resilience to violent storms and hurricanes, Proceedings of the National Academy of Sciences of the United States of America, 113, 64–68, https://doi.org/10.1073/pnas.1510095112, 2016.

Marani, M., D'Alpaos, A., Lanzoni, S., and Santalucia, M.: Understanding and predicting wave erosion of marsh edges, Geophysical Research Letters, 38, https://doi.org/10.1029/2011GL048995, 2011.

Mariotti, G. and Fagherazzi, S.: Modeling the effect of tides and waves on benthic biofilms, Journal of Geophysical Research: Biogeosciences, 117, https://doi.org/10.1029/2012JG002064, 2012.

Mariotti, G. and Fagherazzi, S.: Wind waves on a mudflat: The influence of fetch and depth on bed shear stresses, Continental Shelf Research, 60, S99–S110, https://doi.org/10.1016/j.csr.2012.03.001, 2013.

Mariotti, G., Fagherazzi, S., Wiberg, P. L., McGlathery, K. J., Carniello, L., and Defina, A.: Influence of storm surges and sea level on shallow tidal basin erosive processes, Journal of Geophysical Research: Oceans, 115, C11 012, https://doi.org/10.1029/2009JC005892, 2010.

Martini, P., Carniello, L., and Avanzi, C.: Two dimensional modelling of flood flows and suspended sedimenttransport: the case of the Brenta River, Veneto (Italy), Natural Hazards and Earth System Sciences, 4, 165–181, https://doi.org/10.5194/nhess-4-165-2004, 2004.

Mel, R., Viero, D. P., Carniello, L., Defina, A., and D'Alpaos, L.: Simplified methods for real-time prediction of storm surge uncertainty: The city of Venice case study, Advances in Water Resources, 71, 177–185, https://doi.org/https://doi.org/10.1016/j.advwatres.2014.06.014, 2014.

Molinaroli, E., Guerzoni, S., Sarretta, A., Masiol, M., and Pistolato, M.: Thirty-year changes (1970 to 2000) in bathymetry and sediment texture recorded in the Lagoon of Venice sub-basins, Italy, Marine Geology, 258, 115–125, https://doi.org/https://doi.org/10.1016/j.margeo.2008.12.001, 2009.

Möller, I., Spencer, T., French, J. R., Leggett, D. J., and Dixon, M.: Wave transformation over salt marshes: A field and numerical modelling study from north Norfolk, England, Estuarine, Coastal and Shelf Science, https://doi.org/10.1006/ecss.1999.0509, 1999.

Murray, A. B.: Reducing model complexity for explanation and prediction, Geomorphology, 90, 178–191, https://doi.org/10.1016/j.geomorph.2006.10.020, 2007.

Nicholls, R. J., Lincke, D., Hinkel, J., Brown, S., Vafeidis, A. T., Meyssignac, B., Hanson, S. E., Merkens, J.-L., and Fang, J.: A global analysis of subsidence, relative sea-level change and coastal flood exposure, Nature Climate Change, 11, 338–342, https://doi.org/10.1038/s41558-021-00993-z, 2021.

Park, J., Botter, G., Jawitz, J. W., and Rao, P. S. C.: Stochastic modeling of hydrologic variability of geographically isolated wetlands: Effects of hydro-climatic forcing and wetland bathymetry, Advances in Water Resources, https://doi.org/10.1016/j.advwatres.2014.03.007, 2014.

Pivato, M., Carniello, L., Moro, I., and D'Odorico, P.: On the feedback between water turbidity and microphytobenthos growth in shallow tidal environments, Earth Surface Processes and Landforms, 44, 1192–1206, https://doi.org/10.1002/esp.4567, 2019.

Rodriguez-Iturbe, I., Cox, D. R., and Isham, V.: Some models for rainfall based on stochastic point processes, Proceedings of the Royal Society of London. A. Mathematical and Physical Sciences, 410, 269–288, https://doi.org/10.1098/rspa.1987.0039, 1987.

Sarretta, A., Pillon, S., Molinaroli, E., Guerzoni, S., and Fontolan, G.: Sediment budget in the Lagoon of Venice, Italy, Continental Shelf Research, 30, 934–949, https://doi.org/10.1016/j.csr.2009.07.002, 2010.

Schwimmer, R. A.: Rates and Processes of Marsh Shoreline Erosion in Rehoboth Bay, Delaware, U.S.A., Journal of Coastal Research, 17, 672–683, 2001.

Soulsby, R. L.: Bed shear-stresses due to combined waves and currents, in: Advances in Coastal Morphodynamics, edited by Stive, M. J. F., pp. 420–423, Delft Hydraul., Delft, Netherlands, 1995.

Soulsby, R. L.: Dynamics of Marine Sands: A Manual for Practical Applications, Thomas Telford, London, 1997.

Temmerman, S., Bouma, T. J., Govers, G., and Lauwaet, D.: Flow paths of water and sediment in a tidal marsh: Relations with marsh developmental stage and tidal inundation height, Estuaries, 28, 338–352, https://doi.org/10.1007/BF02693917, 2005.

Tognin, D., D'Alpaos, A., Marani, M., and Carniello, L.: Marsh resilience to sea-level rise reduced by storm-surge barriers in the Venice Lagoon, Nature Geoscience, 14, 906–911, https://doi.org/10.1038/s41561-021-00853-7, 2021.

Tognin, D., Finotello, A., D'Alpaos, A., Viero, D. P., Pivato, M., Mel, R. A., Defina, A., Bertuzzo, E., Marani, M., and Carniello, L.: Loss of geomorphic diversity in shallow tidal embayments promoted by storm-surge barriers, Science Advances, 8, eabm8446, https://doi.org/10.1126/sciadv.abm8446, 2022.

Tognin, D., D'Alpaos, A., D'Alpaos, L., Rinaldo, A., and Carniello, L.: Statistical characterization of erosion and sediment transport mechanics in shallow tidal environments. Part 2: suspended sediment dynamics, Companion paper.

Tommasini, L., Carniello, L., Ghinassi, M., Roner, M., and D'Alpaos, A.: Changes in the wind-wave field and related salt-marsh lateral erosion: inferences from the evolution of the Venice Lagoon in the last four centuries, Earth Surface Processes and Landforms, 44, 1633–1646, https://doi.org/doi:10.1002/esp.4599, 2019.

van Ledden, M., Wang, Z. B., Winterwerp, H., and De Vriend, H. J.: Sand-mud morphodynamics in a short tidal basin, in: Ocean Dynamics, https://doi.org/10.1007/s10236-003-0050-y, 2004.

Wolman, M. G. and Miller, J. P.: Magnitude and frequency of forces in geomorphic processes, The Journal of Geology, 68, 54–74, 1960.

Young, I. R. and Verhagen, L. A.: The growth of fetch limited waves in water of finite depth. Part 1. Total energy and peak frequency, Coastal Engineering, https://doi.org/10.1016/S0378-3839(96)00006-3, 1996.

Zanchettin, D., Bruni, S., Raicich, F., Lionello, P., Adloff, F., Androsov, A., Antonioli, F., Artale, V., Carminati, E., Ferrarin, C., Fofonova, V., Nicholls, R. J., Rubinetti, S., Rubino, A., Sannino, G., Spada, G., Thiéblemont, R., Tsimplis, M., Umgiesser, G., Vignudelli, S., Wöppelmann, G., and Zerbini, S.: Sea-level rise in Venice: historic and future trends (review article), Natural Hazards and Earth System Sciences, 21, 2643–2678, https://doi.org/10.5194/nhess-21-2643-2021, 2021.

Zarzuelo, C., López-Ruiz, A., D'Alpaos, A., Carniello, L., and Ortega-Sánchez, M.: Assessing the morphodynamic response of human-altered tidal embayments, Geomorphology, https://doi.org/10.1016/j.geomorph.2018.08.014, 2018.

Zarzuelo, C., D'Alpaos, A., Carniello, L., López-Ruiz, A., Díez-Minguito, M., and Ortega-Sánchez, M.: Natural and Human-Induced Flow and Sediment Transport within Tidal Creek Networks Influenced by Ocean-Bay Tides, Water, 11, https://doi.org/10.3390/w11071493, 2019.

Zecchin, M., Baradello, L., Brancolini, G., Donda, F., Rizzetto, F., and Tosi, L.: Sequence stratigraphy based on high-resolution seismic profiles in the late Pleistocene and Holocene deposits of the Venice area, Marine Geology, 253, 185–198, https://doi.org/https://doi.org/10.1016/j.margeo.2008.05.010, 2008.

Zhou, Z., Coco, G., van der Wegen, M., Gong, Z., Zhang, C., and Townend, I.: Modeling sorting dynamics of cohesive and non-cohesive sediments on intertidal flats under the effect of tides and wind waves, Continental Shelf Research, 104, 76–91, https://doi.org/https://doi.org/10.1016/j.csr.2015.05.010, 2015.

Zhou, Z., Coco, G., Townend, I., Olabarrieta, M., van der Wegen, M., Gong, Z., D'Alpaos, A., Gao, S., Jaffe, B. E., Gelfenbaum, G., He, Q., Wang, Y., Lanzoni, S., Wang, Z. B., Winterwerp, H., and Zhang, C.: Is "Morphodynamic Equilibrium" an oxymoron?, Earth-Science Reviews, 165, 257–267, https://doi.org/10.1016/j.earscirev.2016.12.002, 2017.

Zhou, Z., Liang, M.-j., Chen, L., Xu, M.-p., Chen, X., Geng, L., Li, H., Serrano, D., Zhang, H.-y., Gong, Z., and Zhang, C.-k.: Processes, feedbacks, and morphodynamic evolution of tidal flat–marsh systems: Progress and challenges, Water Science and Engineering, 15, 89–102, https://doi.org/10.1016/j.wse.2021.07.002, 2022.

Supplement for
Statistical characterization of erosion and sediment transport mechanics in shallow tidal environments. Part 1: erosion dynamics

Andrea D'Alpaos[1,*], Davide Tognin[1,2,*], Laura Tommasini[1], Luigi D'Alpaos[2], Andrea Rinaldo[2,3], and Luca Carniello[2]

[1]Department of Geosciences, University of Padova, Padova, Italy
[2]Department of Civil, Environmental, and Architectural Engineering, University of Padova, Padova, Italy
[3]Laboratory of Ecohydrology ECHO/IEE/ENAC, Ècole Polytechnique Fèdèrale de Lausanne, Lausanne, Switzerland
[*]These authors contributed equally to this work.

Correspondence: Davide Tognin (davide.tognin@unipd.it)

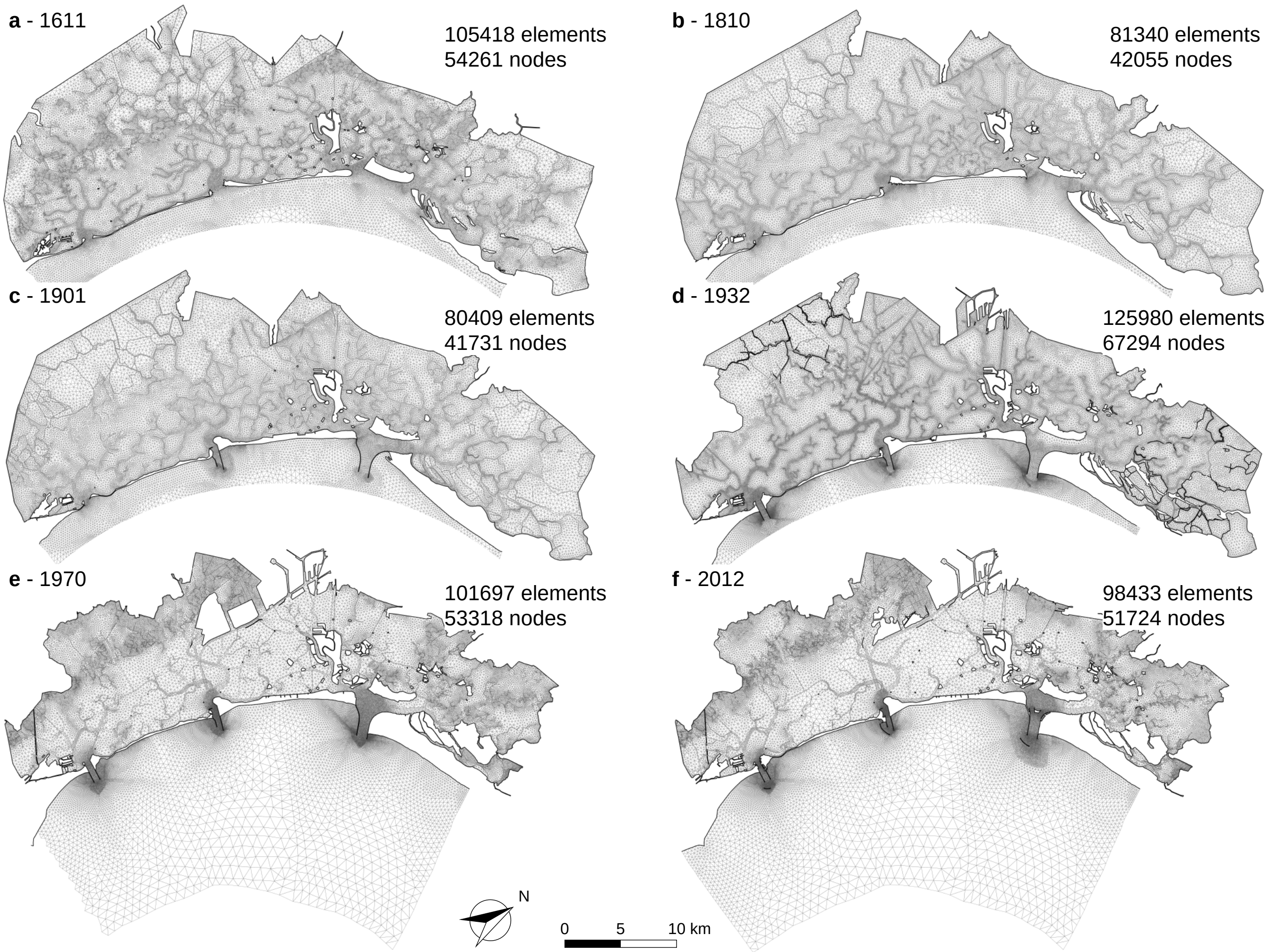

Figure 1. Meshes used in the numerical model. Meshes of the six different configurations of the Venice Lagoon: 1611 (**a**), 1810 (**b**), 1901 (**c**), 1932 (**d**), 1970 (**e**), and 2012 (**f**). For the sake of clarity, the mesh portion representing the sea is shown only in panel (**e**) and (**f**), but it is present in all meshes.

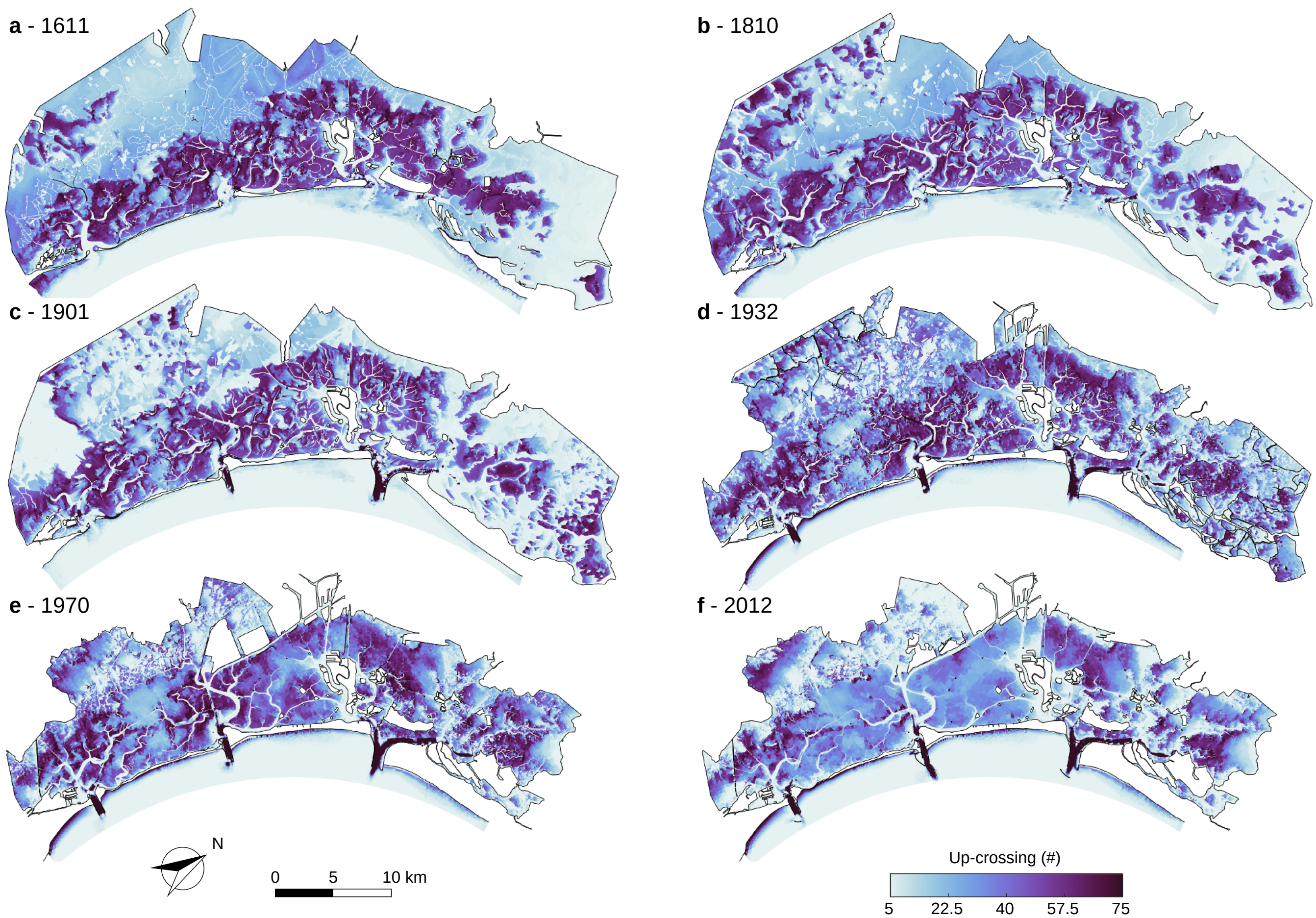

Figure 2. Number of upcrossings of the erosion threshold. Spatial distribution of the number of upcrossings of the threshold for erosion $\tau_c = 0.4$ Pa for the six different configurations of the Venice Lagoon: 1611 (**a**), 1810 (**b**), 1901 (**c**), 1932 (**d**), 1970 (**e**), and 2012 (**f**).

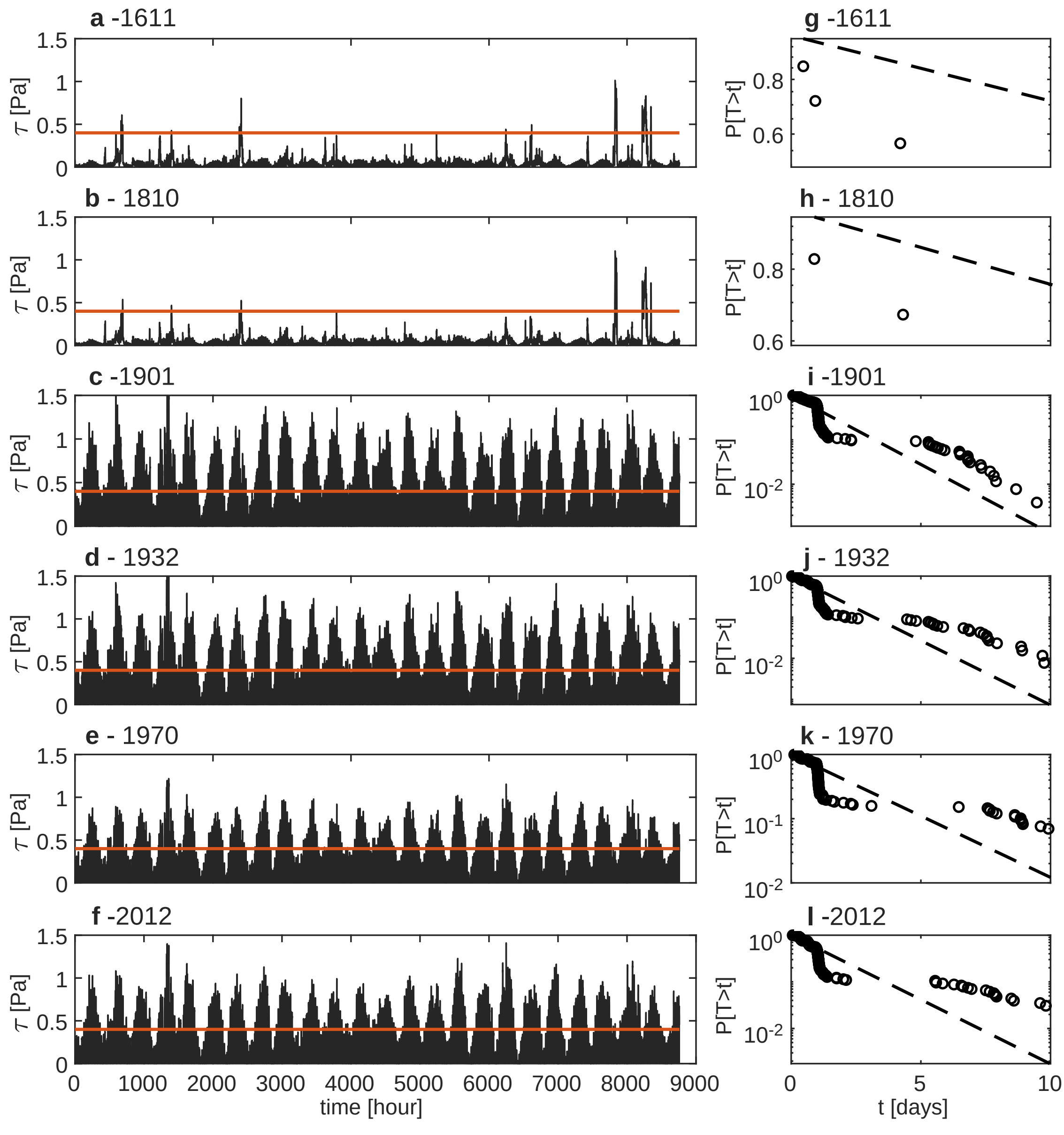

Figure 3. Over-threshold BSS events at the Lido inlet. Statistical analysis at SL station in the Lido inlet: time series of the computed BSS (**a-f**); probability distributions of the interarrival times (circles) and exponential distributions (dashed lines) (**g-l**).

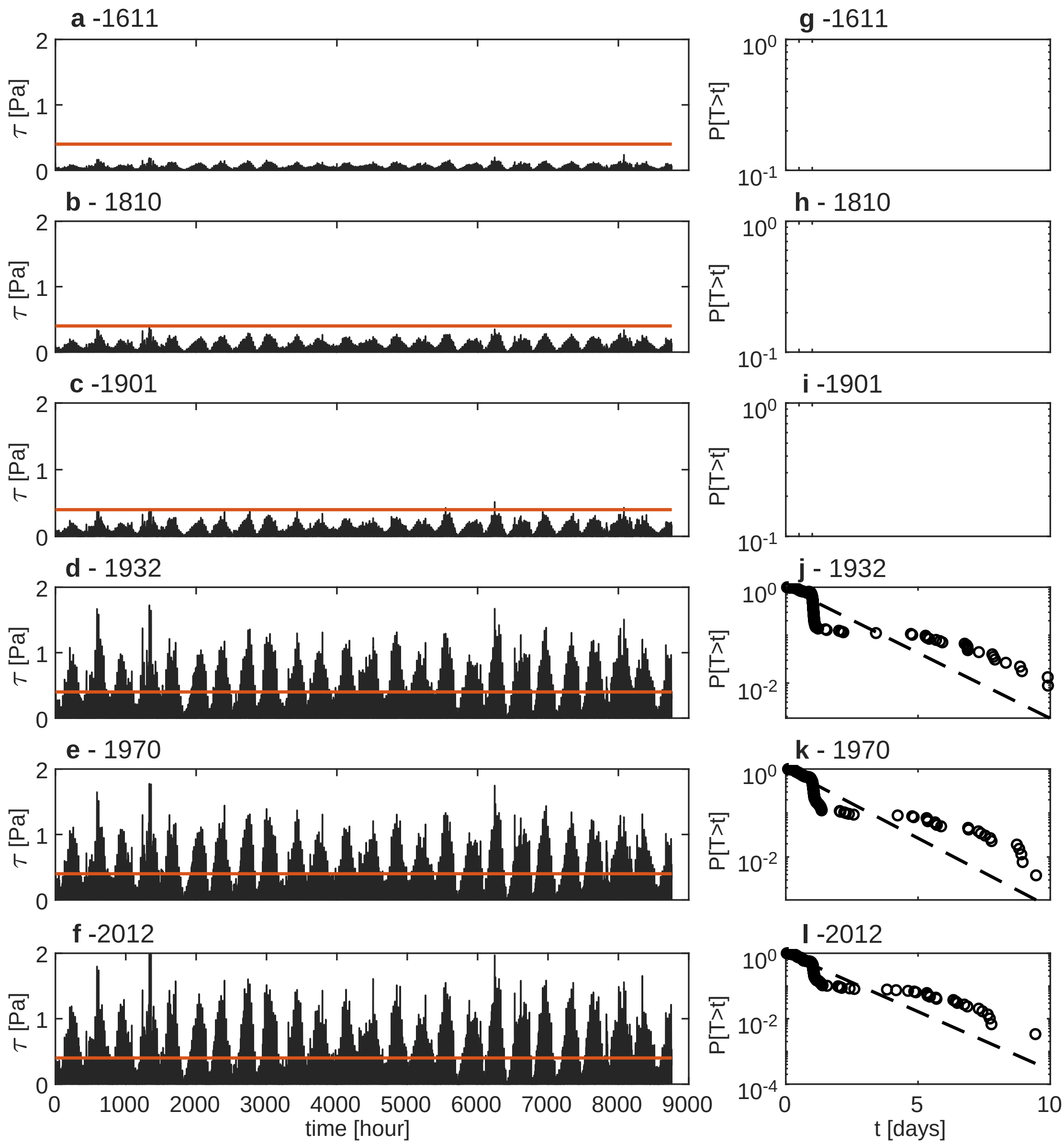

Figure 4. Over-threshold BSS events at the Chioggia inlet. Statistical analysis at SC station in the Chioggia inlet: time series of the computed BSS (**a-f**); probability distributions of the interarrival times (circles) and exponential distributions (dashed lines) (**g-l**).

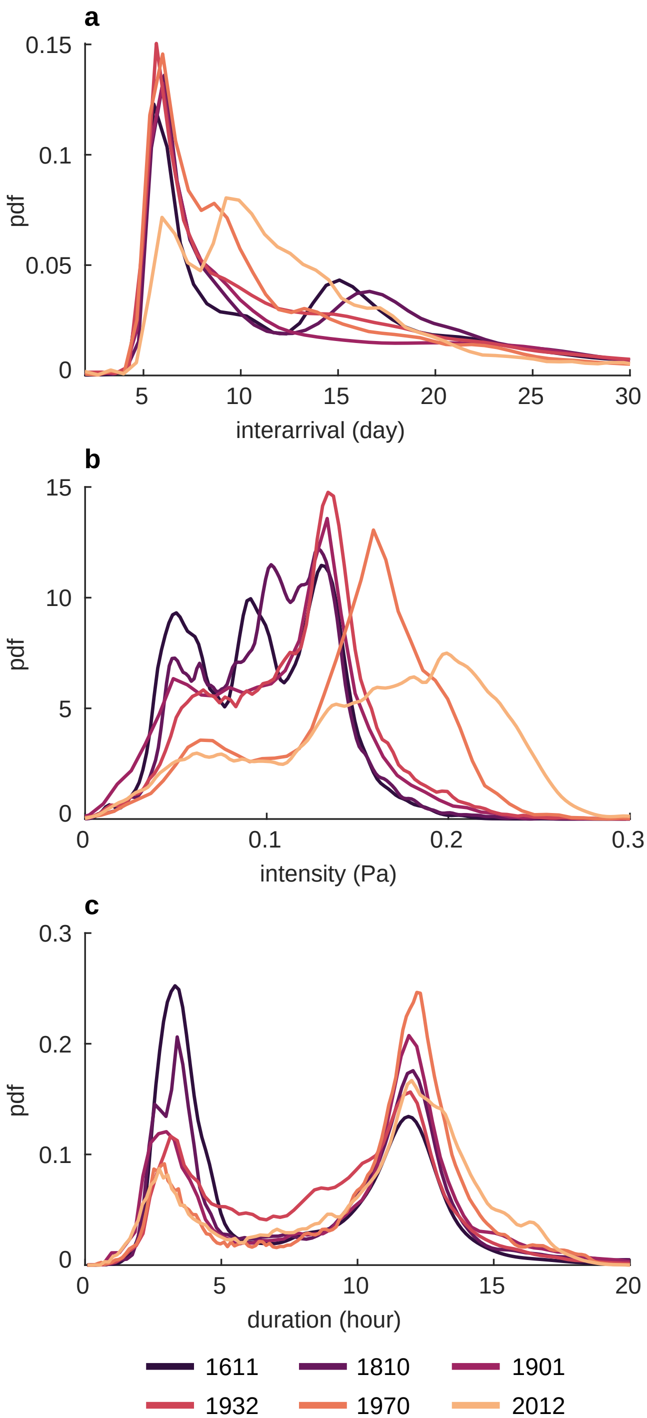

Year	t [day] (mean ± std)	(median)
1611	45.27 ± 76.56	16.29
1810	34.30 ± 61.99	15.69
1901	48.35 ± 80.10	15.14
1932	26.09 ± 40.21	13.17
1970	20.35 ± 32.07	10.07
2012	26.13 ± 42.83	12.67

Year	e [Pa] (mean ± std)	(median)
1611	0.09 ± 0.03	0.09
1810	0.10 ± 0.03	0.10
1901	0.10 ± 0.04	0.11
1932	0.11 ± 0.04	0.12
1970	0.14 ± 0.04	0.15
2012	0.16 ± 0.06	0.16

Year	d [hour] (mean ± std)	(median)
1611	7.54 ± 4.32	6.47
1810	8.84 ± 4.76	10.18
1901	9.67 ± 5.06	11.12
1932	8.95 ± 4.02	9.75
1970	10.36 ± 3.92	11.64
2012	10.27 ± 4.24	11.57

Figure 5. Spatial probability density function of interarrival time, intensity and duration of BSS over-threshold events. Probability density function (left), mean (mean ± standard deviation) and median value (right) of interarrival times t (**a**), intensity e (**b**) and duration d (**c**) of BSS over-threshold events.

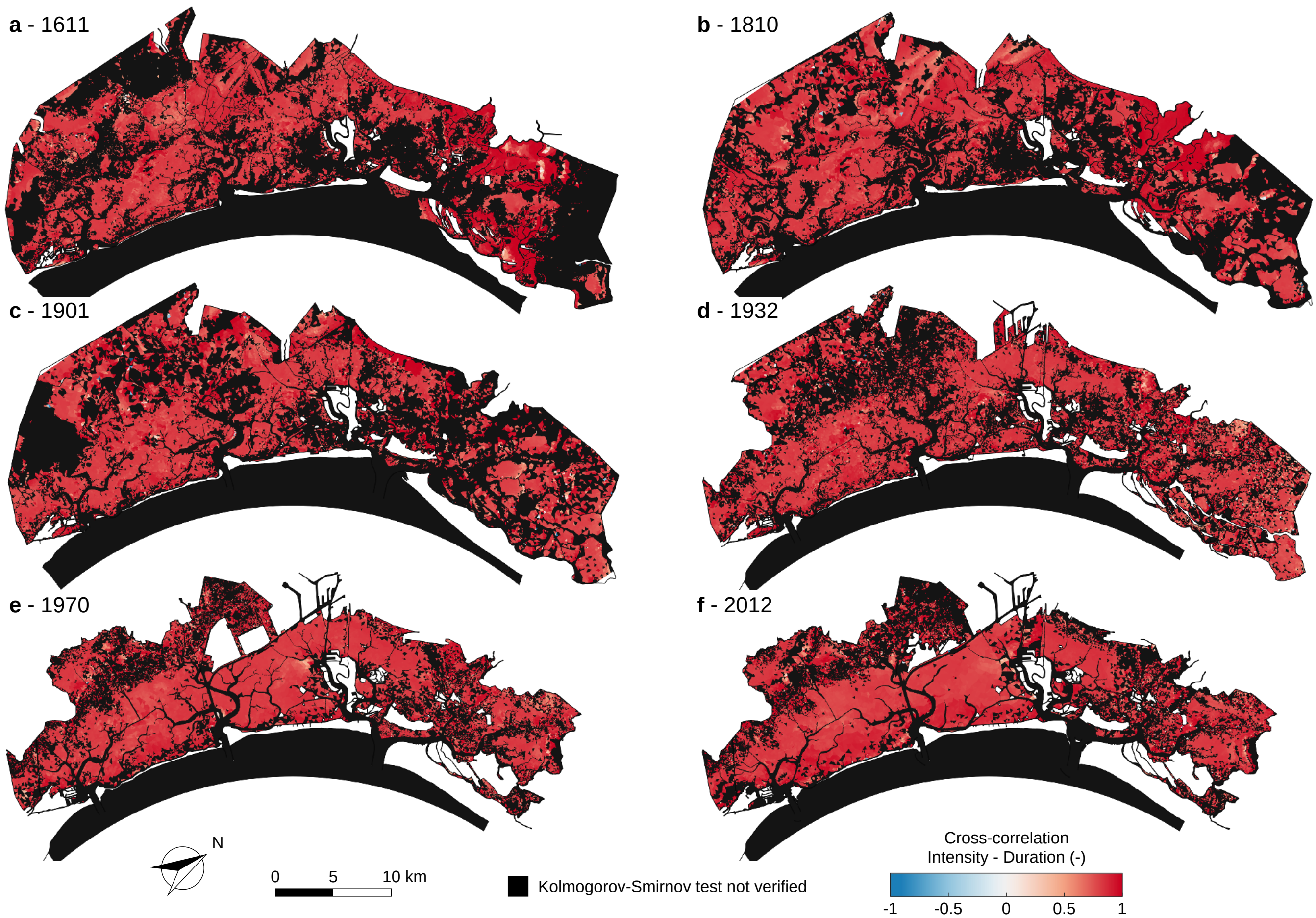

Figure 6. Cross-correlation between intensity and duration of over-threshold BSS events. Spatial distribution of temporal cross-correlation between intensity of peak-excesses and duration of over-threshold exceedances for the six different configurations of the Venice Lagoon: 1611 (**a**), 1810 (**b**), 1901 (**c**), 1932 (**d**), 1970 (**e**), and 2012 (**f**). Black identifies sites where the bottom shear stress cannot be modeled as a marked Poisson process (i.e. the KS test is not verified for the interarrival time).

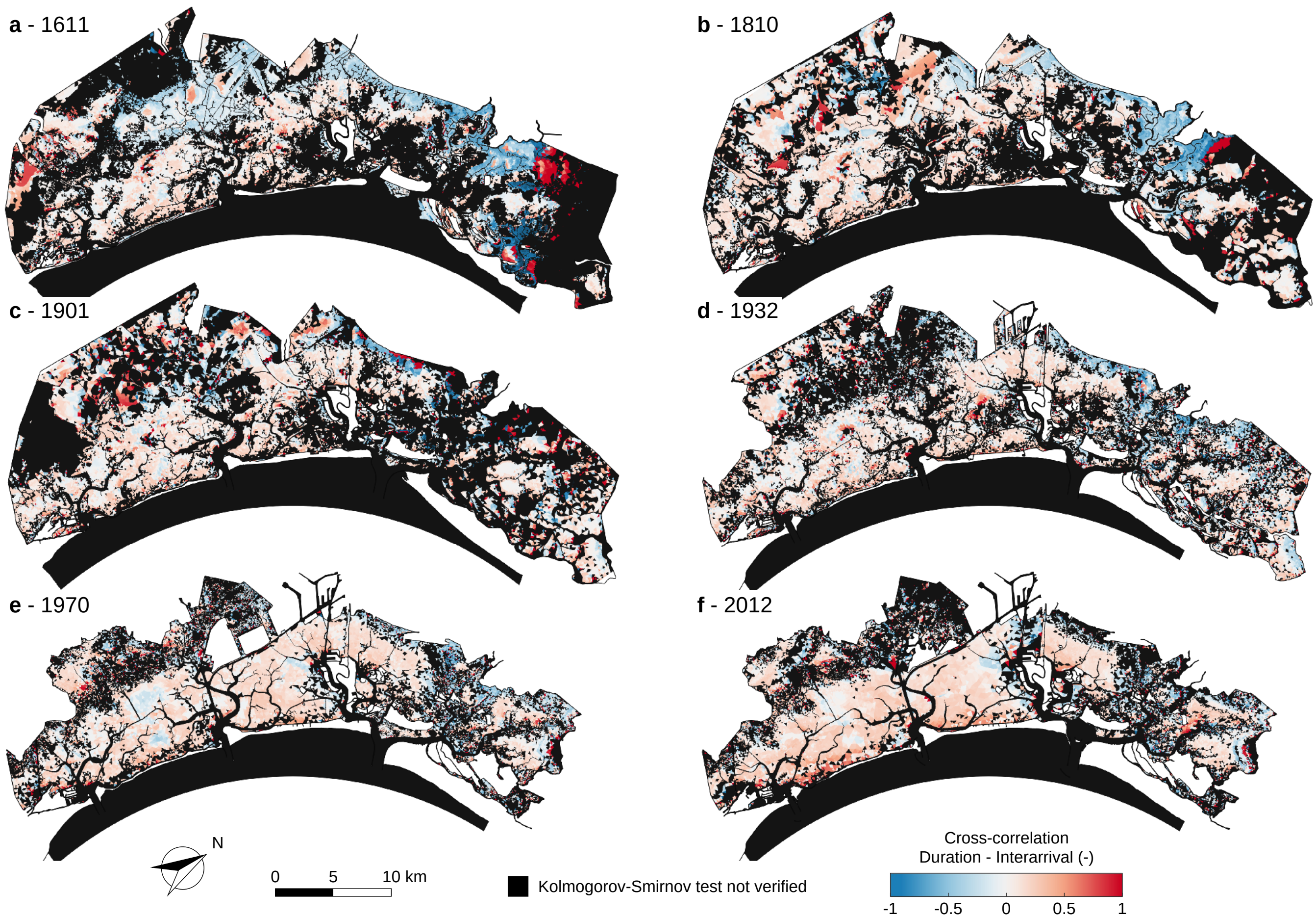

Figure 7. Cross-correlation between duration and interarrival times of over-threshold BSS events. Spatial distribution of temporal cross-correlation between duration and interarrival times of over-threshold exceedances for the six different configurations of the Venice Lagoon: 1611 (**a**), 1810 (**b**), 1901 (**c**), 1932 (**d**), 1970 (**e**), and 2012 (**f**). Black identifies sites where the bottom shear stress cannot be modeled as a marked Poisson process (i.e. the KS test is not verified for the interarrival time).

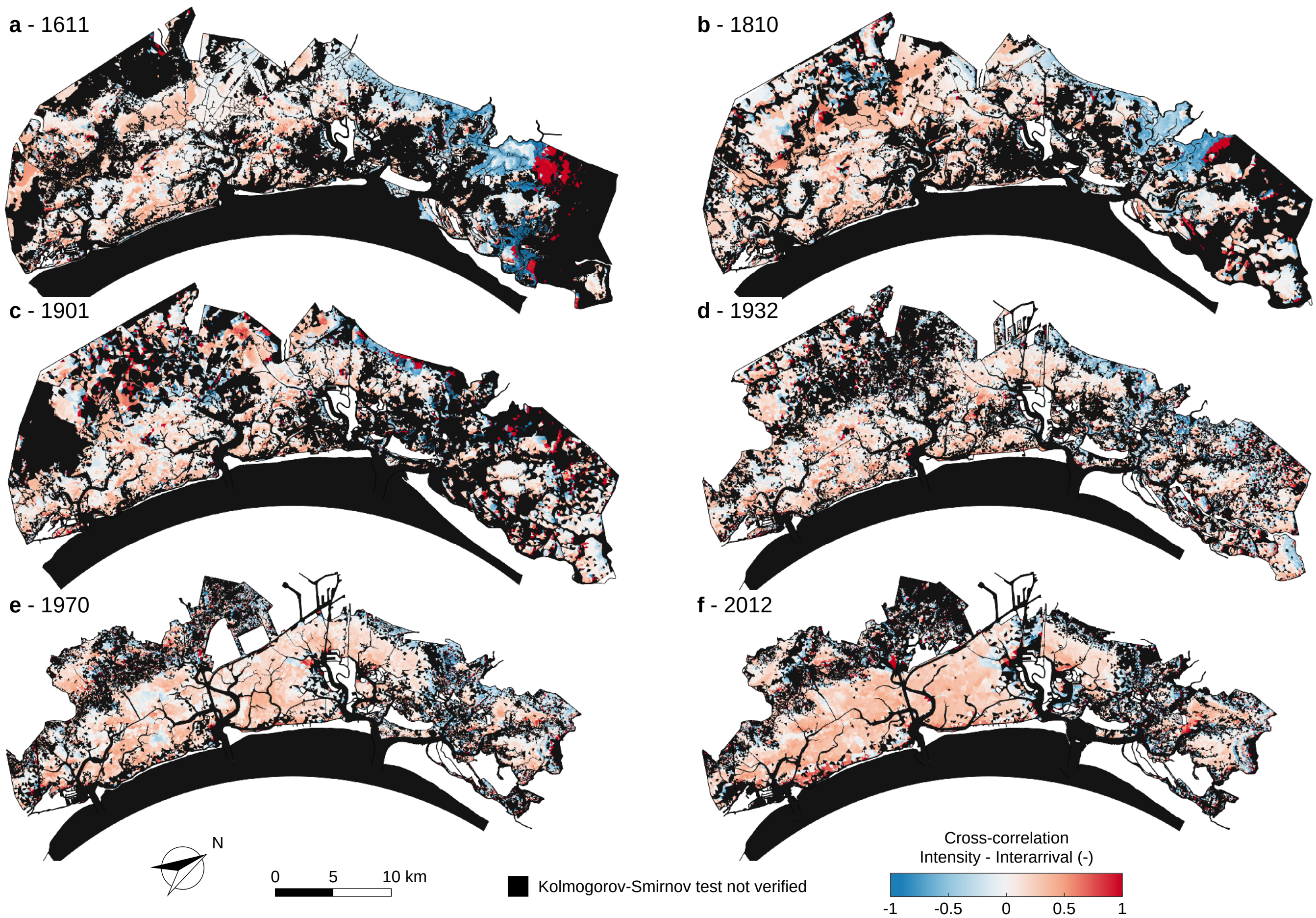

Figure 8. Cross-correlation between intensity and interarrival times of over-threshold BSS events. Spatial distribution of temporal cross-correlation between intensity of peak-excesses and interarrival times of over-threshold exceedances for the six different configurations of the Venice Lagoon: 1611 (**a**), 1810 (**b**), 1901 (**c**), 1932 (**d**), 1970 (**e**), and 2012 (**f**). Black identifies sites where the bottom shear stress cannot be modeled as a marked Poisson process (i.e. the KS test is not verified for the interarrival time) .

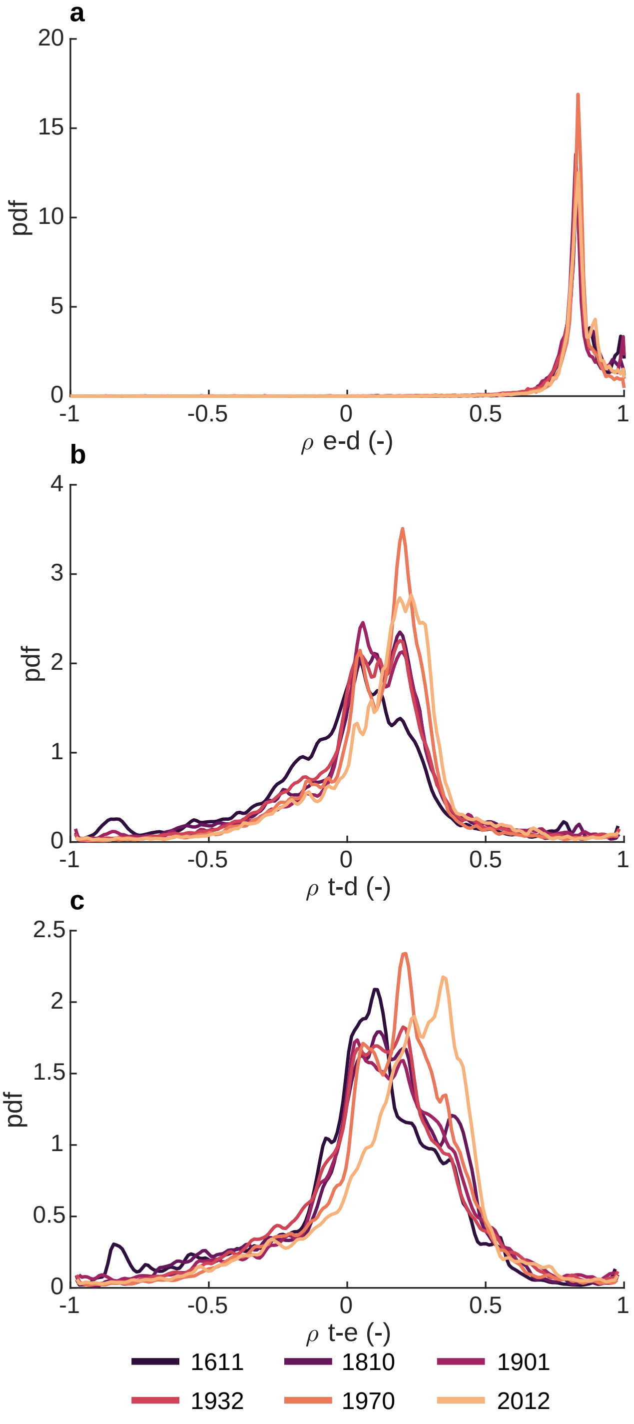

Year	$\rho(e-d)$ [-] (mean $\pm$ std)
1611	0.84 ± 0.09
1810	0.83 ± 0.09
1901	0.82 ± 0.11
1932	0.82 ± 0.11
1970	0.83 ± 0.08
2012	0.83 ± 0.09

Year	$\rho(t-d)$ [-] (mean $\pm$ std)
1611	0.005 ± 0.365
1810	0.069 ± 0.318
1901	0.078 ± 0.356
1932	0.070 ± 0.312
1970	0.105 ± 0.277
2012	0.130 ± 0.308

Year	$\rho(t-e)$ [-] (mean $\pm$ std)
1611	0.05 ± 0.37
1810	0.10 ± 0.33
1901	0.11 ± 0.37
1932	0.10 ± 0.33
1970	0.14 ± 0.30
2012	0.18 ± 0.33

Figure 9. Spatial probability density function of cross-correlation between interarrival time, intensity and duration of BSS over-threshold events. Probability density function (left) and mean value (mean $\pm$ standard deviation, right) of cross-correlation between intesity and duration $\rho(e-d)$ (**a**), interarrival time and duration $\rho(t-d)$ (**b**) and interarrival time and intensity $\rho(t-e)$ (**c**).

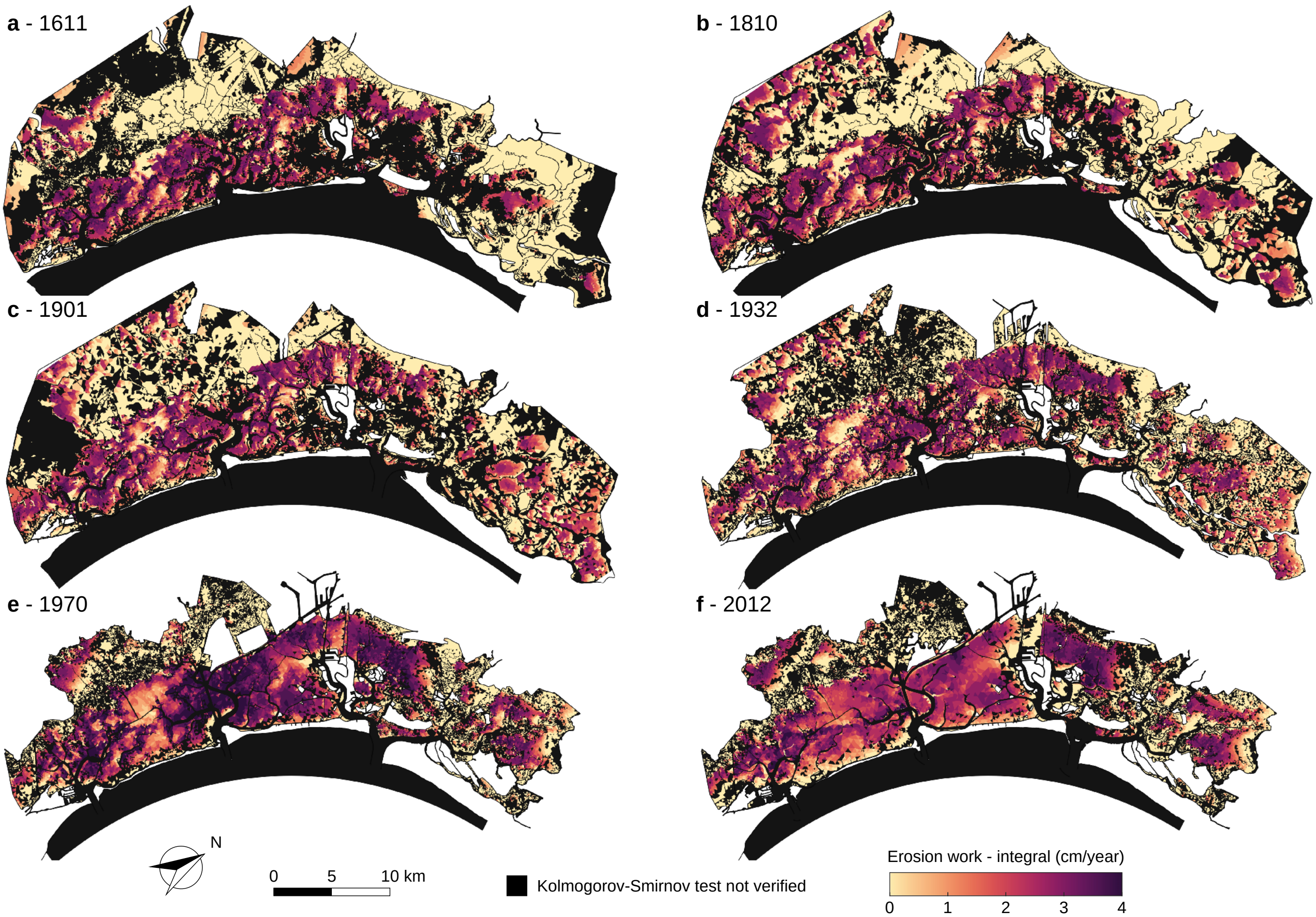

Figure 10. Erosion work computed as integral of over-threshold BSS events. Spatial distribution of erosion work computed with Eq. 2 for the six different configurations of the Venice Lagoon: 1611 (**a**), 1810 (**b**), 1901 (**c**), 1932 (**d**), 1970 (**e**), and 2012 (**f**). Black identifies sites where the bottom shear stress cannot be modeled as a marked Poisson process (i.e. the KS test is not verified for the interarrival time).

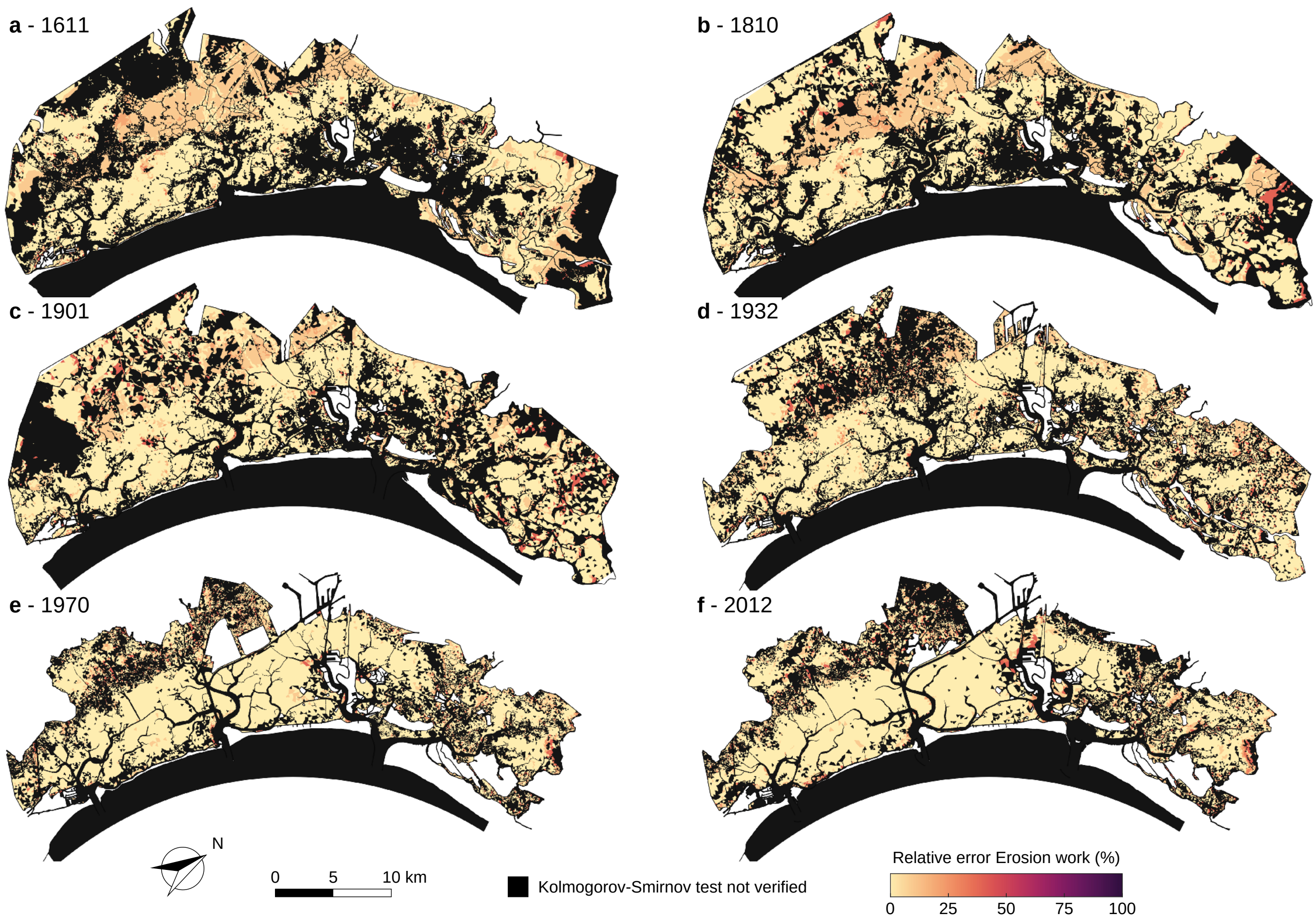

Figure 11. Relative error of synthetic erosion work. Spatial distribution of the relative error between the erosion work calculated with the integral formulation (Eq. 2) and the synthetic one (Eq. 3) for the six different configurations of the Venice Lagoon: 1611 (**a**), 1810 (**b**), 1901 (**c**), 1932 (**d**), 1970 (**e**), and 2012 (**f**). Black identifies sites where the bottom shear stress cannot be modeled as a marked Poisson process (i.e. the KS test is not verified for the interarrival time).